Thesis submitted for the degree of
Candidatus Pharmaciae

Effect of infectious salmon anemia virus (ISAV) infection on expression of apoptosis related genes in Atlantic salmon (*Salmo salar L.*) cells.

By

Kristian Holmen

Department of Pharmaceutical Biosciences
School of Pharmacy
University of Oslo, Norway

December 2006

CONTENTS

1. ACKNOWLEDGEMENTS

The present study was carried out at the School of Pharmacy, Department of Pharmaceutical Biosciences at the University of Oslo, in the period of December 2005 to December 2006.

I would like to thank my supervisor Tor Gjøen for skilful guidance, encouragement and inspiration. Your guidance and help will always be appreciated.

My sincere thanks go to the girls in the virus group, Anne-Lise Rishovd, Ellen Johanne Kleveland and Berit Lyng-Syvertsen, and all colleagues at the department.
A special thank to Berit Lyng-Syvertsen for even offering 24 hour telephone support.

Oslo, February 2007-02-11

Kristian Holmen

2. ABBREVIATIONS

ASK	Atlantic salmon kidney
Cdk	Cyclin dependent kinase
CHSE-214	Chinook salmon embryo cell line
CPE	Cytopathic effect
Ct	Treshold cycle
DHO	Dhori
DNA	Deoxyribonucleic acid
DMSO	Dimethyl Sulphoxide
ds	Double-stranded
EST	Expressed sequence tag
FADD	Fas-associated death domain
FBS	Fetal bovine serum
HA	Hemagglutinin
HE	Hemagglutinin esterase
HEF	Hemagglutinin-esterase-fusion
IAP	Inhibitor of apoptosis
IFN	Interferon
IL	Interleukin
Inf	Influenza
ISA	Infectious salmon anemia
ISAV	Infectious salmon anemia virus
M1	Matrix protein 1
M2	Matrix protein 2
mRNA	message RNA
NA	Neuramidase
NF	Nuclear factor
NK	Natural killer
NP	Nucleoprotein
OD	Optical density
PBS	Phosphate buffered saline
PCR	Polymerase chain reaction

Pdcd5	Programmed cell death 5
p.i	Post infection
REST	Relative Expression Software Tool
RNA	Ribonucleic acid
RNP	Ribonucleoprotein
RT-PCR	Reverse transcription polymerase chain reaction
Segm	Segment
SHK	Salmon head kidney
SS	Staurosporine
ss	Single-stranded
THO	Thogoto
TNF	Tumor necrosis factor
TRAIL	Tumor necrosis factor-related apoptosis inducing ligand

3. ABSRTACT

Infectious salmon anemia virus (ISAV) is the causative agent of an important viral disease threatening the Atlantic salmon aquaculture in Norway and many other countries. Although its structure and pathogenesis is well described little is known about its effects on the expression of genes related to apoptosis in the host cell.

Apoptosis is a genetically controlled process of cell suicide in response to a variety of stimuli and is considered a part of the innate immune response to virus infection, limiting the time and cellular machinery available for viral replication. Previous studies have shown that several RNA viruses induce apoptosis in host-cells. A recent study also suggests that the CPE observed in ISAV-infected SHK-1 and CHSE-214 cells is associated with apoptosis.

Studies of ISAV-induced apoptosis may provide a clearer picture of the cellular mechanisms of viral persistence and pathogenesis in ISAV infection. In the present study we wanted to investigate the effect of ISAV infection on the expression of apoptosis related genes in Atlantic Salmon (*Salmo salar* L.) cells. By using a quantitative real-time PCR approach we analyzed the regulation of key apoptosis related genes during early stages of ISAV infection *in vitro.* Two different permissive cell lines for ISAV were used, Atlantic salmon head kidney (ASK) cells and salmon head kidney (SHK-1) cells.

Our results strongly indicates that IFN-α, Mx and cIAP-1 are up regulated during ISAV infection in both ASK and SHK-1 cell lines. We also showed that viral mRNA increased steadily throughout the infection, in spite of the increased levels of IFN-α and Mx, indicating that these genes have little or no antiviral effect on ISAV in Atlantic salmon cells.

4. INTRODUCTION

4.1 Orthomyxoviridae

The family *Orthomyxoviridae* (from greek *orthos*, "standard, correct" and *myxo*, "mucus") contains five genera, including the influenza A, B and C viruses. A fourth genus, Thogotovirus, includes tick-transmitted orthomyxoviruses (Pringle 1996)and are designated Dhori- and Thogotoviruses. The fifth genera is suggested to be named Aquaorthomyxovirus to reflect the host range of viruses (ISAV) as well as the proposed family allocation (Krossoy, Hordvik et al. 1999). (Figure 4.1)

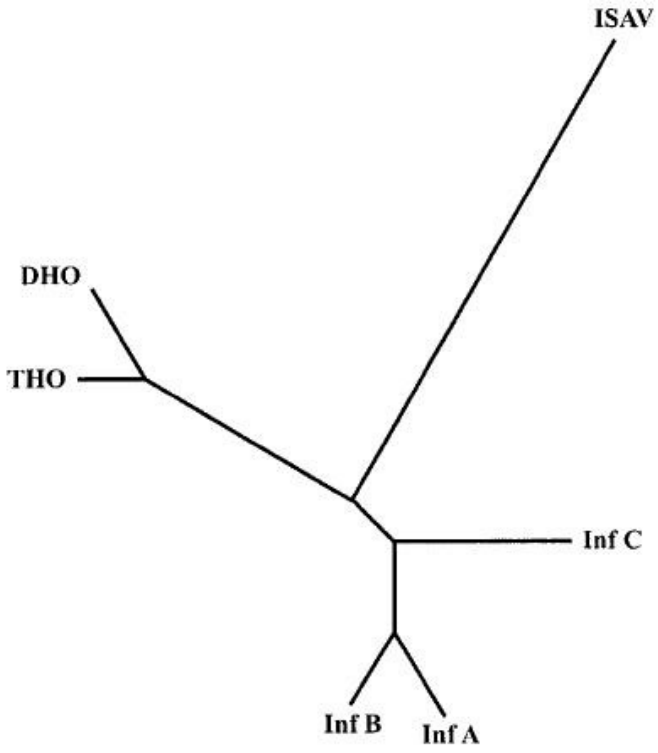

Figure 4.1: Genetic distance tree drawn by the neighbour-joining method. Branch lengths are drawn to scale. Genetic distances were calculated based on the polymerase (PB1) sequences. Virus abbrevations are as follows: Inf A, influenza A/PR/8/34 (J0251); inf B, influenza B/AnnArbor/1/66 (M20170); Inf C, influenza C/JJ/50 (M28060); THO, Thogoto (AF004987); DHO, Dhori (M65866) (Krossoy, Hordvik et al. 1999).

Orthomyxoviridae are single-stranded, enveloped RNA viruses in which the RNA has a negative polarity and is segmented. The genomic RNA of negative strand RNA viruses serves two functions: first as a template for synthesis of messenger RNAs (mRNAs) and second as a template for synthesis of the antigenome (+) strand, which is a copy of the complete viral genome (for influenza virus, often termed template RNA or complementary RNA (cRNA)). Negative strand RNA viruses encode and package their own RNA transcriptase, but mRNAs are only synthesized once the virus has been uncoated in the infected cell. Viral replication occurs after synthesis of the mRNAs and requires the continuous synthesis of viral proteins. The newly synthesized antigenome (+) strand serves as the template for further copies of the (-) strand. (Lamb 2001)

ISAV, influenza A and B viruses have their RNA divided into 8 segments, whereas influenza C only has 7 segments (Mjaaland, Rimstad et al. 1997; Cox, Brokstad et al. 2004), and the tick-borne viruses, Dhori virus and Thogoto virus, have 6 segments (Leahy, Dessens et al. 1997). The most conserved orthomyxoviroid gene has been shown to be the RNA-dependent RNA polymerase (PB1) (Lin, Roychoudhury et al. 1991). The occurrence of consensus regions in the RNA-dependent RNA polymerase has led to the assumption that the sequence similarities may be linked to the existence of a common ancestral genetic element bearing a polymerase function, which emerged only once during the evolution (Krossoy, Hordvik et al. 1999).

4.1.1 Virion structure

The lipid membrane of orthomyxoviruses is derived from the plasma membrane of the host cell. Influenza virus A and B are distinguished by two integral membrane glycoproteins, hemagglutinin (HA) and neuramidase (NA), that protrude from the virion surface. HA is responsible for attachment of the virus to sialic acid-containing oligosaccharides on the host cell surface and also fusion between the viral and endosome membranes resulting in release of viral RNPs into the cytoplasma. The NA cleaves sialic acids and plays important roles in viral entry and release. Influenza C virus, by contrast, has only a single membrane glycoprotein, hemagglutinin-esterase-fusion protein (HEF). HEF does not recognize sialic acid, but facilitates binding of virus to the host by binding to oligosaccharides containing a terminal 9-α-acetyl-N-acetylneuramidase acid. The receptor-destroying enzyme (esterase) of influenza C virus resides in the HEF protein, at a site distinct from that responsible for receptor binding.

Within the lipid envelope are the matrix (M1) protein and RNA segments, which are associated nucleoprotein (NP) and three large polymerase proteins, designated PA, PB1 and PB2 on the basis of their overall acidic or basic amino acid composition. The complexes of viral RNA, NP, PA, PB1 and PB2 are termed ribonucleoprotein (RNP) (Kawaoka 2001). A third integral membrane protein is the ion channel formed by the matrix (M2) protein in influenza A viruses and NB in influenza B viruses (Cox, Brokstad et al. 2004). As illustrated in Figure 4.2, both RNA segment 7 and 8 code for more than one protein (M1 and M2, and NS1 and NS2, respectively). The nonstructural protein, NS1, binds to double stranded RNA, preventing activation of the interferon-induced protein kinase R, suggesting a role of this protein in the prevention of interferon-mediated antiviral responses. NS2 associates with RNP through interaction with the C-terminal portion of M1 protein. (Kawaoka 2001)

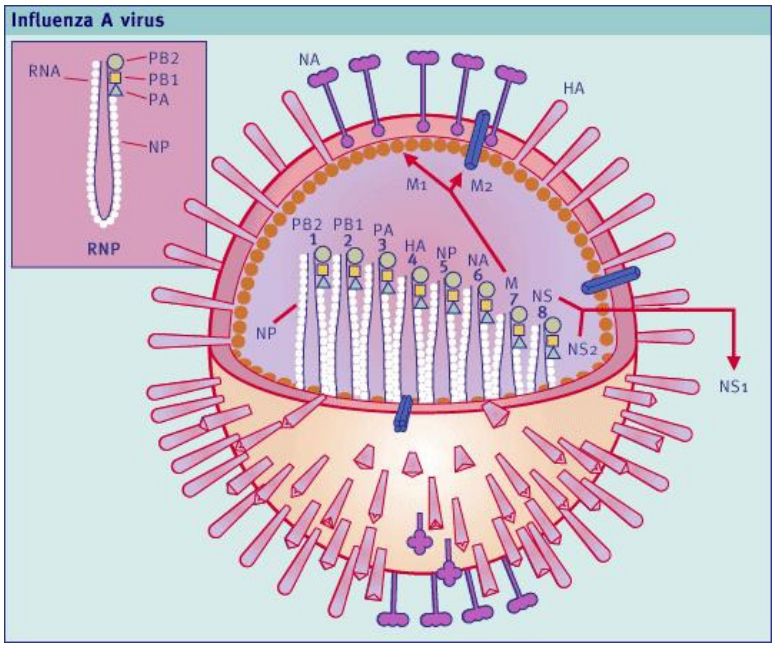

Figure 4.2: Schematic representation of an influenza A viral particle. The virion contains a lipid envelope in which three different types of proteins are anchored: the hemagglutinin (HA), the neuramidase (NA) and the M_2 protein. Inside the envelope there is a protein layer constituted by the M_1 protein (filled ring) which surrounds the viral core or ribonucleoproteins (RNPs). RNA segments exists in a circular conformation stabilized by base-pairing between their 3' and 5' ends. Eight different RNA segments can be found per virion. (Picture taken from http://www.vetscite.org/publish/articles/000041/img0002.jpg)

4.2 Infectious salmon anemia virus

Infectious salmon anemia (ISA) was first described as a disease entity in juvenile Atlantic Salmon, *Salmo Salar L*., in Norway in 1984 (Thorud and Djupvik 1988). ISA first appeared in the North Atlantic (Lovely, Dannevig et al. 1999), and was later recognized in salmon farms on the Atlantic coast of Canada and USA, Scotland and Faeroes (Bouchard, Keleher et al. 1999; Lovely, Dannevig et al. 1999). ISA outbreaks have also been reported in Pacific Coho Salmon (*Oncorhyncus kisutch*) in Chile (Kibenge, Garate et al. 2001).

The infectious salmon anemia virus (ISAV) was determined to be the causative agent of infectious salmon anemia, an important disease threatening Atlantic salmon aquaculture industry on the Northern hemisphere (reviewed in (Rimstad and Mjaaland 2002; Kibenge, Munir et al. 2004)). In 1994 a long term cell line, developed from Atlantic salmon head kidney macrophages (SHK-1), that supported the growth of ISAV was established (Dannevig, Falk et al. 1995). The SHK-1 cell line allowed replication of ISAV with development of cytopathic effects (CPE). A reverse transcriptase polymerase chain reaction (RT-PCR) technique has been developed for detecting ISAV, in which a fragment of the ISAV genome is being amplified (Mjaaland, Rimstad et al. 1997).The pathological changes of the disease include exophthalmia, pale gills, ascites, hemorrhagic liver necrosis, renal interstitial hemorrhage and tubular nephrosis.

The transmission of ISAV in farmed populations of Atlantic salmon will be difficult to control, because ISAV has shown that it can infect and replicate in wild fish like: sea trout, brown trout, rainbow trout, eels, herring (*Clupea barengus*) and Artic char (*Salvelinus alpinus*), resulting in asymptomatic, probably lifelong, carriers of the virus (Krossoy, Hordvik et al. 1999){Kibenge, 2004 #55. ISAV is a commercially important *Orthomyxovirus* and recurrent infectious diseases causes considerable economically losses in aquaculture farming.

4.2.1 Virion structure

ISAV shares several morphological, biochemical and physiochemical features with influenza viruses. It is the only species of the Isavirus geneus, one of the five genera of the family *Orthomyxoviridae* {Krossoy, 1999 #49}. ISA virus are enveloped particles of 90-140 nm in diameter (Dannevig, Falk et al. 1995; Dannevig, Falk et al. 1995) with 13-15 nm long muchroom-shaped surface projections. These surface proteins consists of a combination of receptor-binding hemagglutinin and receptor-destroying enzyme activity that has been demonstrated to be an esterase, designated HE (Falk, Aspehaug et al. 2004).

The genome is composed of eight segments of linear, single-stranded negative sense RNA (as do the influenza A and B viruses) ranging in length from 1.0 to 2.4 kb with a total molecular size of approximately 14.3 kb (Clouthier, Rector et al. 2002). All the eight RNA segments of ISAV have been sequenced (Mjaaland, Rimstad et al. 1997; Krossoy, Hordvik et al. 1999; Rimstad, Mjaaland et al. 2001; Ritchie, Heppell et al. 2001; Clouthier, Rector et al. 2002; Ritchie, Bardiot et al. 2002). The genomic segment 1 encoded product is assumed to correspond to PB2 of the influenza viruses. Genomic segment 2 encodes for the PB1 part of the viral RNA polymerase. The PB1 protein is the most conserved protein of orthomyxoviruses. Comparison of the ISAV PB1 protein sequence with that of other Orthomyxoviridae revealed amino acid identities 20.8%-24.1% (Krossoy, Hordvik et al. 1999). The amino acid sequence encoded by the open reading frame (ORF) of segment 3 was identified to be the nucleoprotein (NP) (Ritchie, Heppell et al. 2001). And segment 4 encodes for PA, which seems to be the acidic part of the viral polymerase (Ritchie, Heppell et al. 2001). Segment 5 encodes the glycoprotein gp50 that has been shown to be a membrane fusion protein which requires proteolytic cleavage to induce fusion (Aspehaug, Mikalsen et al. 2005). Segment 6 encodes HE and segment 7 and 8 have two overlapping ORFs. This arrangement is similar to that of the influenza A virus. ISAV share many typical properties with the Orthomyxoviridae but they also have a few differences from the other Orthomyxoviruses, such as: they are pathogenic for aquatic species and have a lower optimum growth temperature, between 10 and 15 ºC. There is no virus replication at temperatures above 25 ºC.

The order of the genome segments encoding the proteins in ISAV appears to differ from those in influenza viruses (se table 4.1).

Genome segment	Gene products[1]	
	Isavirus	*Influenzavirus A*
1	PB2 (84 kDa)[2]	PB1 (96 kDa)
2	PB1 (84 kDa)	PB2 (87 kDa)
3	NP (77 kDa)	PA (85 kDa)
4	PA (71 kDa)	HA_1 (48 kDa), HA_2 (29 kDa)
5	gp50 (47 kDa)	NP (50–60 kDa)
6	HE (42 kDa)	NA (48–63 kDa)
7	p32 (32 kDa), NEP (18 kDa), p11 (11 kDa)	M1(25 kDa), M2 (15 kDa)
8	M1 (24 kDa), NS1 (16 kDa)	NS1(25 kDa), NS2 (12 kDa)

Table 4.1: Comparison of genome coding assignments for Isavirus and Influenza A virus.
PB2, PB1 and PA, polymerase; NP, nucleoprotein; HA, hemagglutinin; Gp50 is an envelope fusion glycoprotein (Aspehaug, Mikalsen et al. 2005); HE, hemagglutinin esterase in ISAV (Falk, Aspehaug et al. 2004); NA, neuramidase; M1, matrix protein (Falk, Aspehaug et al. 2004); p32, a structural protein of unknown function in ISAV; M2, ion channel protein; p11, protein of unknown status and function; NS1, non-structural protein 1; NS2, non-structural protein 2 (also known as nuclear export protein, NEP)
Table taken from (Kibenge, Munir et al. 2004).

4.3 Apoptosis

Apoptosis (derived from the Greek word for a natural process of leaves falling from trees) is a fundamental biological process that is implicated in early development such as during metamorphosis in insects and amphibians, and organogenesis in virtually all multicellular organisms. Apoptosis is an essential component of the homeostasis of normal tissue. For instance, it plays an active part in the removal of tissue between fingers and toes during embryonic development (Meier, Finch et al. 2000)and in the formation of T and B cell repertoires of the immune system by eliminating non- or self-reactive cells (Krammer 2000). Apoptosis also exerts a role opposite to mitosis in the maintenance of cells populations. As many as 10^{11} cells die in an adult human per day to ensure tissue homeostasis, and it is estimated that within a typical year, the mass of cells a person loses through cell death is almost equivalent to their entire body weight. Such death therefore probably plays an important role in dynamic processes such as tissue remodeling and responses to stress. Apoptosis is also a protective mechanism, directing lysis of virus infected cells, foreign cells or incipient neoplasm (Wu 2001).

Cell death may occur through at least two broadly defined mechanisms: necrosis or apoptosis (Kerr, Wyllie et al. 1972). Necrosis is a passive, catabolic, pathological cell death process which generally occurs in response to external toxic factors such as inflammation, ischemic or toxic injury. It is not thought to ever occur under physiological conditions. Necrosis is characterized by swelling of mitochondria, early rupture of the plasma membrane, dispersed chromatin and early destruction of the intact structure of the cell (Wu 2001), which result in spilling of cell contents causing a potentially damaging inflammatory response (Alberts, Johnson et al. 2002).

By contrast, a cell that undergoes apoptosis dies neatly, without damaging its neighbors. Apoptosis is a form of active, metabolic, genetically encoded and evolutionary selected death pathway, which features characteristic morphological and biochemical alterations such as cell shrinkage, condensation of nuclear chromatin with internucleosomal fragmentation of deoxyribonucleic acid (DNA), disintegration into membrane wrapped fragments and exposure of phosphatidylserine residues on the cell surface (Müllauer 2006). Degradation of chromosomal DNA into oligonucleosome-sized fragments results in a distinct laddering pattern on an ethidium bromide-stained agarose gel that represents a hallmark for apoptosis (Wyllie 1980). The appearance of phosphatidylserine molecules on the surface of apoptotic cells, by a flip-flopp movement of phospholipid molecules in the lipid bilayer of the

plasma membrane (Martin, Reutelingsperger et al. 1995), help macrophages to recognize the dying cells and to eliminate them by phagocytosis. This prevents leaking of the cytoplasmic contents into the intercellular space, minimizing tissue inflammation, avoiding damage to neighboring cells and resulting in efficiently degradation of host (or viral) DNA.

4.3.1 Genes involved in apoptosis

Many genes involved in the execution of apoptosis have been identified, and different, although strongly interacting, pathways of apoptosis signaling have been dissected (Reed 2000). (Figure 4.3)

Extrinsic pathways use transmembrane death receptors such as Fas (CD95), tumor necrosis factor-related apoptosis inducing ligand (TRAIL) receptors 1 and 2, and tumor necrosis factor (TNF) receptors 1 and 2. Engagement of the receptors with their cognate ligands leads to formation of a death-inducing signaling complex, with recruitment of the adapter protein FADD (Fas-associated death domain), which creates a link to initiator procaspases 8 and 10, proteases that contain an active-site cysteine and cleave proteins after certain aspartate residues. Activated caspases 8 and 10 then promote cleavage of downstream effector caspases 3, 6 and 7 that degrades various cellular proteins, ultimately leading to apoptosis. The chain of protease activation (caspases cascade) can be interrupted by inhibitor of apoptosis proteins (IAPs), which block the activity of caspases (Deveraux and Reed 1999).

An intrinsic apoptosis pathway focuses on mitochondria and is triggered by various types of cellular stress (e.g withdrawal of growth factors, hypoxia, cytotoxic drugs) that lead to a change in the permeability of the outer mitochondrial membrane with leakage of mitochondrial proteins into the cytosol. Cytochrome c is an important protein, which when released, binds to the cytosolic adapter molecule Apaf-1 and induces its oligomerization (Kroemer and Reed 2000). Oligomerized Apaf-1 recruits the initiator procaspase 9, which after activation triggers a cascade of caspases reactions. Another protein released from mitochondria HtrA2/Omi, has the ability to block IAPs and promotes cell death via its serine protease activity. Other proteins released from the mitochondria are AIF, which translocates to the nucleus and induces chromatin condensation and EndoG nuclease, which fragments DNA.

The mitochondrial branch of apoptosis signaling is regulated by the bcl-2 family. Some members of this family, like bcl-2 itself or bcl-X_L, inhibit apoptosis, at least partly by blocking the release of cytochrome c from mitochondria. Other members of the bcl-2 family are not death inhibitors, but instead promote procaspase activation and cell death. Some of these apoptosis promoters, such as Bad, function by binding to and inactivating the death-inhibiting members of the family, whereas others, like Bax and Bak, stimulate the release of cytochrome c from mitochondria. Bax and Bak are themselves activated by other apoptosis-promoting members of the bcl-2 family, such as Bid (Alberts, Johnson et al. 2002). Pro- and

antiapoptotic Bcl-2 family members form homo- and heterodimers and their relative concentration determines the susceptibility to apoptotic stimuli (Gross, McDonnell et al. 1999).

A second intrinsic apoptosis pathway features the nuclear protein p53. The molecule links cell damage to cell cycle arrest and apoptosis. It is activated in the response to DNA damage or cell stress and arrests cells with DNA damage by promoting genes that induce cell cycle arrest (especially p21, which inactivates cyclin-Cdk complexes necessary for the cell to progress through the cell cycle) or initiates apoptosis, partially by inducing the transcription of proapoptotic genes like Bcl-2 associated X protein (BAX) and genes whose products generate reactive oxygen species (Vogelstein, Lane et al. 2000).

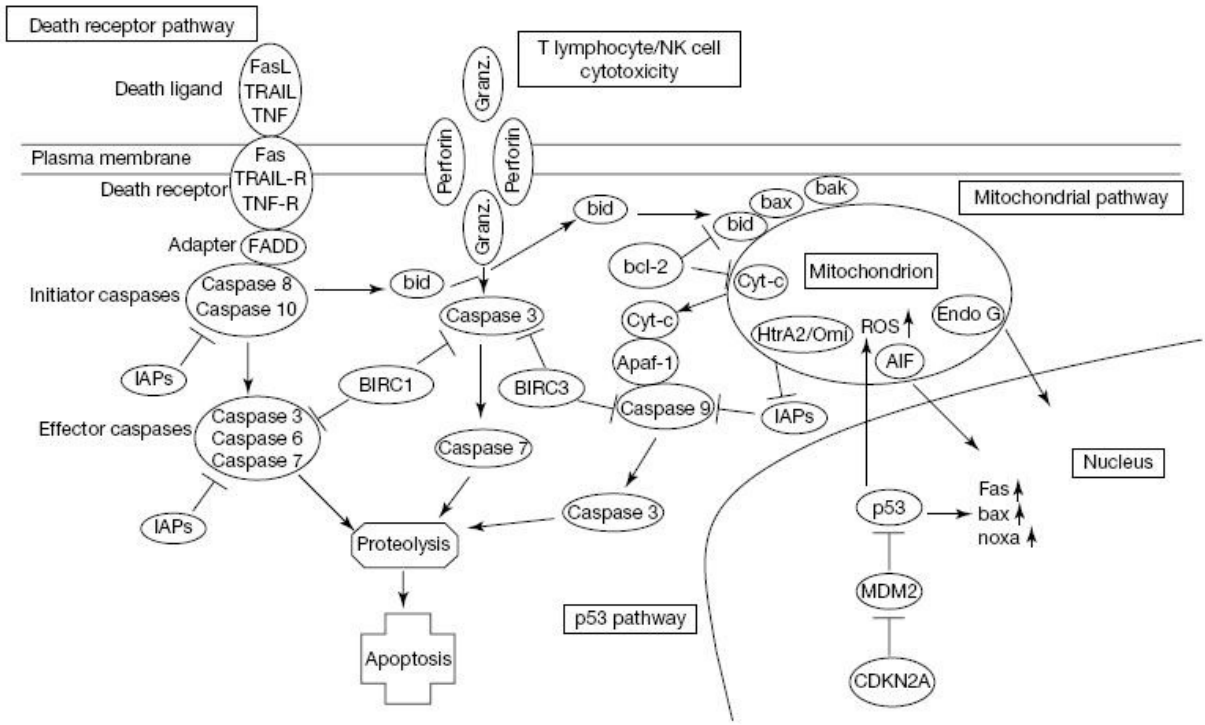

Figure 4.3: Simplified scheme of the major apoptosis signaling pathways (see text for details). IAPs: inhibitor of apoptosis proteins; Cyt-c: cytochrome-c; Granz: granzyme; NK: natural killer; ROS: reactive oxygen species; BIRC1/2: inhibitor of apoptosis proteins (Müllauer 2006)

4.3.2 Genes analyzed

IFN-α

Interferons are transcriptionally regulated cytokines and key players in the innate antiviral immune response. The transcription of IFN is induced by the presence of double stranded RNA and causes an antiviral state in neighboring cells (reviewed in (Bonjardim 2005)). More details of IFN-actions are discussed in section 4.3.3.

MX

Mx-proteins are interferon induced GTPases, which have an antiviral activity against a wide range of RNA viruses, including o*rthomyxoviruses*. In the case of orthomyxoviruses, mx proteins prevent the incoming viral nucleocapsids from being transported into the nucleus, the site of viral transcription and replication. As a consequence, these viral components are trapped and sorted to locations where they become unavailable for the generation of new virus particles (Haller and Kochs 2002).

p53

"intrinsic stresses" such as oncoproteins, direct DNA damage, hypoxia and survival factor deprivation, can initiate the intrinsic apoptotic pathway through the activation of p53. Activated p53 can then either initiate cell cycle arrest by promoting genes that induce cell cycle arrest (e.g. p21), or induce apoptosis by transcriptionally activating proapoptotic Bcl-2 family members (e.g. Bax and Bak) and repressing antiapoptotic Bcl-2 proteins (Bcl-2, Bcl-X_L) and IAPs. p53 may also induce apoptosis by activating genes whose products generate reactive oxygen species (ROS) (Johnstone, Ruefli et al. 2002).

cIAP-1

The inhibitor of apoptosis (IAP) family consists of a number of evolutionary conserved proteins first discovered in Baculoviruses. In addition to suppressing apoptotic cell death, IAPs are involved in an increasing number of other cellular functions, including cell cycle and intracellular transduction. It has been shown that cIAP-1 inhibits apoptosis by directly binding and inhibiting cell death proteases, caspase-3 and -7. cIAP-1 can also prevent

the proteolytic processing of procaspases-3, -6, and -7 by inhibiting the cytochrome-c-induced activation of procaspases-9 (Chang, Cheng et al. 2006).

pdcd5

Programmed cell death 5 (pdcd5) gene, previously named TF-1 apoptosis-related gene 19 (TFAR19), is a novel apoptosis-related gene cloned in 1999 from TF-1 human leukemic cell line undergoing apoptosis. The human pdcd5 gene encodes a protein that shares significant homology with the corresponding protein of species ranging from yeast to mice. The level of pdcd5 protein expressed in cells undergoing apoptosis is significantly increased compared with control cells. The appearance of pdcd5 in the nuclei of apoptotic cells precedes the externalization of phosphatidylserine and fragmentation of chromosomal DNA. The nuclear translocation of pdcd5 is a universal event of the apoptotic process, and may be a novel early marker for apoptosis (Chen, Sun et al. 2001).

bcl2l

The bcl2l gene encodes a Bcl-X_L-like protein with antiapoptotic effects. After an apoptotic stimulus, Bcl-X_L appears to localize primarily to the mitochondrial outer membrane where it might bind other apoptotic factors such as Bad and Bax or form an ion channel thought to maintain the integrity of the mitochondrial membrane and thus hindering the release of cytochrome c (Chen, Gong et al. 2001; Alberts, Johnson et al. 2002).

Caspase-3

Caspases are a family of cysteine proteases that play important roles in regulating apoptosis. Caspase-3 is one of three highly homologous caspases (caspase-3, -6 and -7) that form the execution subfamily (effector caspases). It has been shown that depletion of caspase-3 in a cell-free apoptotic system inhibited most of the downstream events, including various substrate cleavages, DNA fragmentation, chromatin marginalization, etc, whereas elimination of either caspase-6 or -7 had no effect. Thus, caspase-3 is important for the execution of certain, but not all, specific downstream events of apoptosis (Degterev, Boyce et al. 2003).

4.3.3 Viruses and apoptosis

The objectives for all viruses are to infect target cells, replicate large numbers of progeny virions, and spread these progeny to initiate new rounds of infections. Viruses encode highly efficient proteins to optimize such replication; however, target organisms possess both systemic and cell-based defenses to limit virus infection, including immune and inflammatory processes and execution of suicide of infected cells. In the face of such powerful host defense mechanisms, most viruses have evolved proteins that are able to inhibit or delay protective actions until sufficient viral yields have been produced. Such viral proteins, which have been created either by convergent evolution or by the capture of host sequences encoding entire proteins or individual functional domains, ablate the host response by targeting strategic points in defense pathways. In addition, some viruses appear to encode products that actively induce apoptosis as part of an exit strategy to enhance virus spread.

Multicellular organisms have a variety of host defenses against viral infection (Roulston, Marcellus et al. 1999). Systemically, the first line of defense is generally a cell-mediated immune response. This involves the generation of cytokines such as interleukin 1 (IL-1) and TNF, which activates macrophages, NK cells that induces apoptosis in infected cells, and neutrophils that then phagocytize and help to clear the infected cells. The second line of defense is mediated through the humoral immune response and involves cytotoxic T cells, antibodies generated from B cells, and numerous cytokines that regulate their response. The third level of defense exists at the cellular level. Induction of interferon by the presence of viral nucleic acids (usually double stranded RNA) can curtail the spread of infection by inducing an antiviral state in neighboring cells. Interferons (IFN) have two modes of action that lead to the shut down of viral protein synthesis (reviewed in (Samuel 2001)). First interferons lead to the activation of RNase-L that degrades viral mRNA. Second, interferons also induce the synthesis of PKR, a double-strand-RNA-dependent kinase. Activated PKR leads to a series of downstream events including phosphorylation of the translation initiator factor eIF-2α, activation of Nuclear Factor (NF)-κB and transcriptional induction of numerous pro-apoptotic genes including those encoding Fas, p53 and Bax (Gil and Esteban 2000). Another major outcome of IFN is the synthesis of MX protein which is a potent inhibitor of influenza virus replication (Penny and Stuart-Harris 2001). Se figure 4.4 for cellular responses to IFN signals.

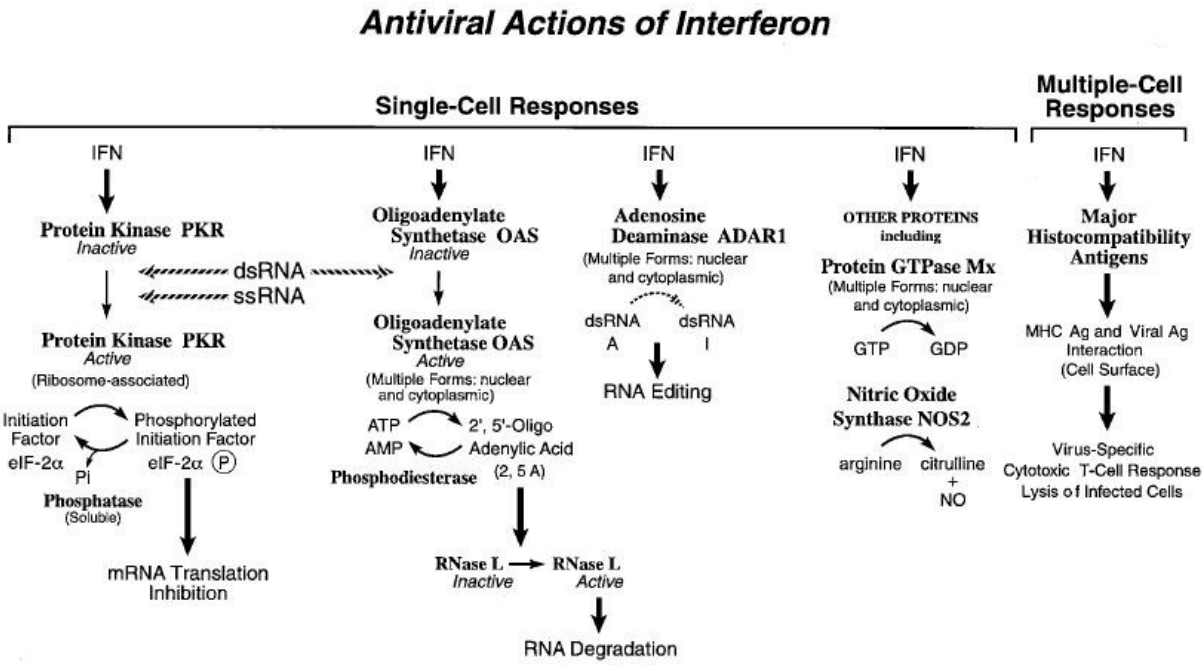

Figure 4.4: Functions of selected IFN-inducible proteins believed to affect virus multiplication. PKR kinase inhibits translation initiation through the phosphorylation of protein synthesis initiation factor eIF-2Aα. OAS synthetase family and the RNase L nuclease mediate RNA degradation. The family of MX protein GTPases appear to target viral nucleocapsids and inhibit RNA synthesis. ADAR which edits double-stranded RNA by deamination of adenosine to yield inosine. IFN induced expression of MHC class I and II antigens and NOS may contribute to the antiviral response observed within whole animals (Samuel 2001).

A critical step in viral pathogenesis is the ability of a virus to inhibit host antiviral responses through the inhibition of host gene expression and/or by interfering with programmed cell death. Viruses has developed various strategies either to promote or inhibit apoptosis, or even to do both at different stages in their replication cycle in the host cell (reviewed by (Roulston, Marcellus et al. 1999)). Influenza A virus is known to induce apoptosis both *in vivo* and *in vitro* in the latest stages of infection. Influenza virus infection induces the expression of Fas, and Fas-mediated apoptosis has been suggested as an important mechanism of cell death during influenza virus infection. The role of Fas in influenza A virus induced apoptosis is supported by the activation of caspases 8, but no caspases 9, in virus infected cells. The Fas expression by influenza virus or dsRNA is mediated partly by the dsRNA-dependent protein kinase (PKR), indicating the involvement of the host antiviral response in the induction of apoptosis during influenza A infection (Balachandran, Roberts et al. 2000). Caspase mediated cleavage of nucleocapsid prodein (NP) of human strains of influenza A also supports the antiviral role of apoptosis during influenza virus infection (Zhirnov, Konakova et al. 1999). The role of various viral proteins during influenza virus

induced apoptosis has also been studied. It has been shown that NS1 (non-structural) protein is capable of inducing apoptosis when expressed in cell cultures (Schultz-Cherry, Dybdahl-Sissoko et al. 2001). Experiments in Madin Darby canine kidney (MDCK) cells demonstrated that neuramidase (NA) could activate latent transforming growth factor beta to its biologically active form, a broad inducer of apoptosis (Morris, Price et al. 1999). Inhibitors of NA delayed the onset of apoptosis when added shortly after infection. Also viruses with highly active NA induced apoptosis in host cell than did those with less active NA (Morris, Price et al. 1999). Interaction of M1 (matrix) protein of influenza A virus with cellular caspase-8 suggests that M1 protein may have a role in virus-induced apoptosis (Zhirnov, Ksenofontov et al. 2002). A new influenza virus gene product, PB-F2, has also been shown to play important roles in influenza induced apoptosis (Chen, Calvo et al. 2001). It has been suggested that ISAV induces apoptosis in SHK-1 cells via activation of the caspase pathway, and that the ISAV putative PB2 protein and proteins encoded by RNA segment 7 bound caspase-8 specifically *in vitro*, suggesting that these viral proteins may have a role in ISAV induced apoptosis (Joseph, Cepica et al. 2004).

4.4 Real-Time Polymerase Chain Reaction

The real-time, fluorescence-based reverse transcription polymerase chain reaction (RT-PCR) is the most sensitive method for detection of low-abundance mRNA, often obtained from limited tissue samples. It has become the method of choice for detecting mRNA (Bustin 2000), and is of particular value for expression studies in fish because availability of antibodies is still limited. Three diagnostic assays are in widespread use for ISAV diagnosis, which include virus isolation on permissive cell lines such as SHK-1 (Dannevig, Falk et al. 1995), indirect fluorescent antibody testing (Falk, Namork et al. 1998) and reverse transcriptase polymerase chain reaction (Mjaaland, Rimstad et al. 1997). Of these assays, the RT-PCR is generally regarded as the most sensitive (Devold, Krossoy et al. 2000; Snow, Raynard et al. 2003). Recent development in real-time PCR technology offer the potential to overcome many of the limitations of conventional PCR including an improved sensitivity of ISAV diagnostics. Indeed, a sensitivity increase of 100-fold over conventional RT-PCR was recently reported using a SYBR green-based assay for the detection of ISAV (Munir and Kibenge 2004).

Several factors have contributed to the transformation of this technology into a mainstream research tool: (i) as a homogeneous assay it avoids the need for post-PCR processing, (ii) a wide ($> 10^7$-fold) dynamic range allows a straight forward comparison between RNAs that differ widely in their abundance, and (iii) the assay realises the inherent quantitative potential of the PCR, making it a quantitative assay as well as a qualitative assay (Gibson, Heid et al. 1996; Heid, Stevens et al. 1996; Ginzinger 2002).

4.4.1 Theory of Real-time PCR

Real-time PCR is the technique of collecting data throughout the PCR reaction as it occurs, thus combining amplification and detection into a single step. This is achieved using different fluorescent chemistries that correlate PCR product concentration to fluorescence intensity. Reactions are characterized by the point in time (or PCR cycle) where the target amplification is first detected. This value is usually referred to as the cycle threshold (C_t), the time at which fluorescence intensity is greater than background fluorescence. Consequently, the greater the quantity of target DNA in the starting material, the faster a signal will appear, yielding a lower C_t (Heid, Stevens et al. 1996).

PCR can be divided into four major phases (figure 4.5) (Tichopad, Dilger et al. 2003):

- The linear ground phase (usually during the first 10-15 cycles) is in the beginning of the PCR reaction, and fluorescence emission at each cycle has not yet risen above background.
- The early exponential phase is where the amount of fluorescence starts to rise above background.
- The log-linear phase is where the PCR reaction reaches its optimal amplification period with the PCR product doubling after every cycle in ideal reaction conditions.
- The plateau stage is reached when the reaction components become limited. The PCR-reaction is no longer doubling its products after every cycle.

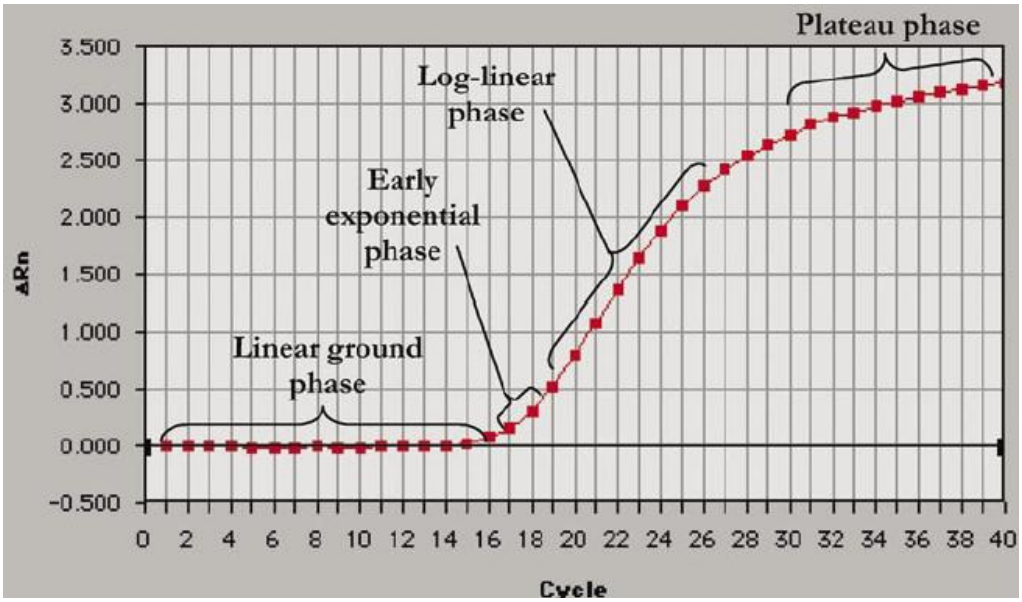

Figure 4.5: Phases of the PCR amplification curve. The PCR amplification curve charts the accumulation of fluorescent emission at each reaction cycle. Data gathered from these phases are important for calculating background signal, cycle threshold and amplification efficiency. Rn is the intensity of fluorescent emission of the reporter dye divided by the intensity of fluorescent emission by the passive dye (a reference dye incorporated into the PCR master mix to control for differences in master mix volume). This graph is copied from (Wong and Medrano 2005).

The 7000 System SDS Software Version 1.2.3 (Applied Biosystems) sets baseline and cycle threshold automatically based on the data gathered from these phases.
During the linear ground phase baseline fluorescence is being calculated.
The cycle threshold value (C_t) is usually set when the reaction have reached a threshold where it is significantly higher (usually 10 times the standard deviation of the baseline) than background fluorescence. This occurs in the log-linear phase where the PCR amplification is working ideally. This value is representative of the starting copy number in the original template and is used to calculate experimental results (Heid, Stevens et al. 1996).

When quantifying mRNA, real-time PCR can be performed in two different ways. Either as a one-step reaction, where the entire reaction form cDNA synthesis to PCR amplification is performed in a single tube, or as a two-step reaction, where reverse transcription and PCR amplification occurs in separate tubes (Wong and Medrano 2005).

The general steps performed during a real-time PCR, from RNA isolation to data analysis is outlined in figure 4.6.

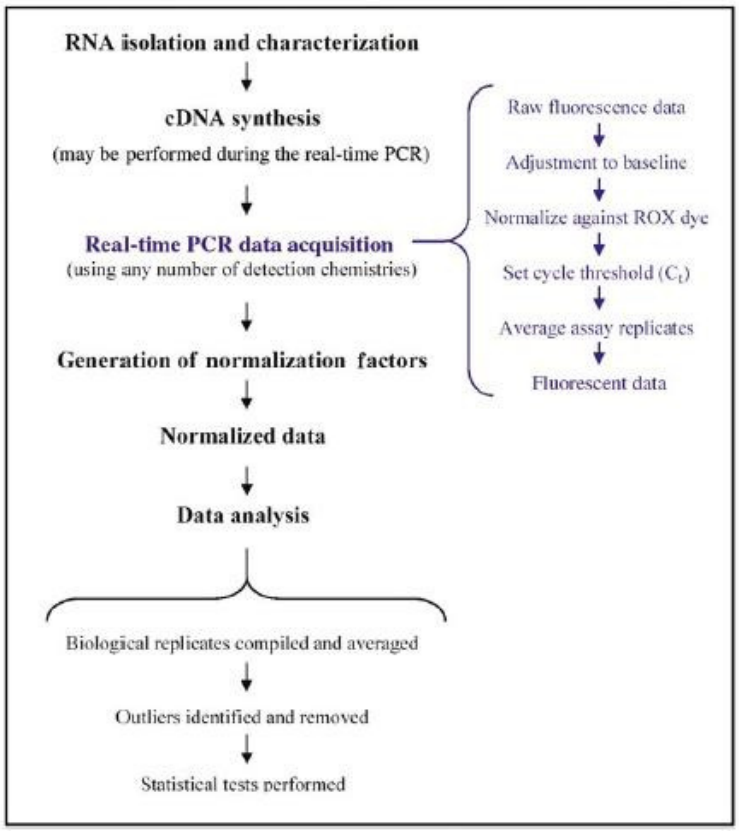

Figure 4.6: Steps performed when measuring gene expression using real-time PCR. This figure is copied from (Wong and Medrano 2005).

One-step real time PCR is thought to minimize experimental variation because both enzymatic reactions occur in a single tube. However, this method uses mRNA as a starting template, which is prone to rapid degradation if not handled properly. Therefore a one-step reaction may not be suitable in assays where the sample is tested on several different occasions over a period of time. One-step protocols are also reportedly less sensitive than two-step protocols (Battaglia, Pedrazzoli et al. 1998).

Two-step real-time PCR separates the reverse transcription reaction from the real-time PCR assay, allowing several different real-time PCR assays on dilutions of a single cDNA. Because the process of reverse transcription has highly variable reaction efficiencies (Reinhold, Berkin et al. 2001), using dilutions from the same cDNA template ensures that reactions from subsequent assays have the same amount of template as those earlier. A two-step protocol may be preferred when using a DNA binding dye (such as SYBR Green I) because its easier to eliminate primer-dimers through the analysis of melting curve temperatures (T_m) (Vandesompele, De Paepe et al. 2002). However, two-step protocols allow for increased opportunities of DNA contamination in real-time PCR, due to more sample handling.

4.4.2 Detection chemistries

There are several different fluorescence detection chemistries available, but in this study we used SYBR Green I, a DNA binding dye as mentioned earlier. DNA binding dyes is thought to bind to the minor grove of dsDNA (figure 4.7). In its unbound state it has relatively low fluorescence but when bound to DNA it shows strong emission. As the dsDNA accumulates during PCR cycling, more dye can bind and emit fluorescence. Thus, the fluorescence intensity increases proportionally to dsDNA concentration (Wittwer, Herrmann et al. 1997).

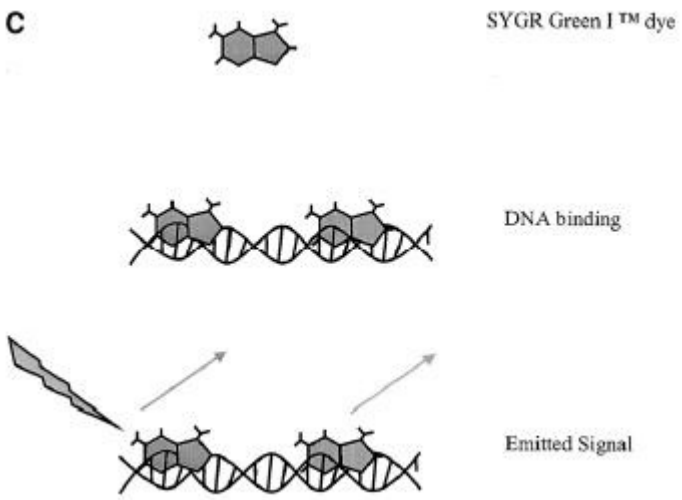

Figure 4.7: SYBR Green I DNA binding Dye. SYBR Green I binding to dsDNA and emitting a fluorescent signal. Figure copied from (Ginzinger 2002).

Using DNA binding dyes is a very flexible technique because one dye can be used for different gene assays.

PCR master mix volume has been shown to be a factor in PCR amplification efficiency such that differences in master mix volume in reactions using the same amount of starting template have different reaction efficiencies (Liu and Saint 2002). A passive reference dye (such as ROX) is often included in the master mix to account for subtle differences in PCR master mix volumes as well as non-PCR related fluctuations in fluorescence signal.

4.4.3 Relative Quantification

Relative quantification describes the changes in expression of the target gene relative to some reference group such as an untreated control or a sample at time zero in a time course study (Livak and Schmittgen 2001). Errors in quantification of mRNA transcripts are easily affected by any variation in the amount of starting material between samples. A frequently used strategy to compensate for these errors is to amplify, simultaneously with the target gene, a nonregulated housekeeping gene that serves as an internal reference against which other RNA values can be normalized (Karge, Schaefer et al. 1998). In this study 18S and EF1α where used as reference genes (Jorgensen, Kleveland et al. 2006).

To ensure that normalisation strategies are applied with proper statistical validity, mathematical models for real-time PCR quantification, such as REST 2005 (relative expression software tool)(Pfaffl, Horgan et al. 2002), have been developed and are used to analyze the real-time PCR results. The purpose of REST 2005 is to determine whether there is a significant difference between samples and controls, while taking into account issues of reaction efficiency and reference gene normalisation.

5. MATERIALS

5.1 Reagents and chemicals

Applied Biosystems, Warrington, UK

- SYBR® GREEN PCR Master Mix

Arcus, Oslo, Norway

- Ethanol

Bio Whittaker, Wokingham, UK

- Fetal bovine serum (FBS, Australian orgin)
- Gentamicin (50mg/ml)
- Leibowitz (L-15) medium

Cambrex Bio Science Rockland, ME, USA

- FlashGel™ DNA Marker
- FlashGel™ Loading Dye

Eppendorf, Hamburg, Germany

- Water, Molecular Biology Grade)

Gibco BRL, Uxbridge, UK

- 2-mercaptoethanol (2-ME) (50mM)
- L-glutamine (200mM)
- Trypsin-EDTA

Merck, Darmstadt, Germany

- HCl
- KCl
- KH_2PO_4
- NaCl

- $Na_2HPO_4 \cdot 2H_2O$

Sigma, St. Louise, USA

- Staurosporine Ready Made Solution
- DMSO

5.2 Kits

RNeasy® Mini Kit (Qiagen, MD, USA)
RNase free DNase set (Qiagen, MD, USA)
TaqMan® Reverse Transcription Reagents (Applied Biosystems, NJ, USA)
FlashGel™ System Kit (Cambrex Bio Science Rockland, ME, USA)

5.3 Solutions

PBS, pH 7,4 (4 L)

32 g	NaCl
0,8 g	KCl
1,08 g	KH_2PO_4
7,12 g	$Na_2HPO_4 \cdot 2H_2O$
3950 ml	Deionized water.

pH adjusted to 7,4 with HCl.
Autoclaved, and stored at + 4 ºC.

20% Sucrose solution (100 ml)

20 g	Sucrose
ad 100 ml	Deionized water

5.4 Primers

Genes	Direction	Sequence	Amplicon	Acc.no
cIAP-1 a	F	GGCGTAATGACGACGTGAAGT	101	**tc43301**
	R	CCTAGGGAACCATTTGGCGT		
cIAP-1 b	F2	GGTGGTTGTGTCGGCTCTG	101	
	R2	CTCGGCCAGCATCTCTTTCT		
Pdcd5 a	F	AGGCCAAACAGAGGGAAACA	101	**tc29121**
	R	TGGCTTCACCAGAGCCAAGT		
Pdcd5 b	F2	AACCGACGAAAGGTGATGGA	101	
	R2	CCTGAATCCCTCCCTAAGCC		
bcl2l a	F	TTGTCAGTTGGTGCTGGAGG	101	**tc29759**
	R	CCAAATTGCTTCTGCCGTTC		
bcl2l b	F2	AAGCCATTGCAAATGGGTCT	101	
	R2	TGCTGCTTTCACTGCCTCAA		
cIAP-1(2) a	F	CAGAACAGCCCGTTGCTCAT	101	**BG934097**
	R	CGAGCGAAGGTGGAGATACG		
cIAP-1(2) b	F2	AGAACAGCCCGTTCCTCATG	101	
	R2	CCGAGCGAAGGTGGAGATAC		
Caspase 3 a	F	GGAATGAGCTTTCGCAATGG	101	**DQ008069**
	R	ACAGTCTGGTCATTGGCAACC		
Caspase 3 b	F2	TCAGTGCAAAGGTTTACGACAGA	101	
	R2	ACACACTGACCAAGGCTGGG		
p53	F	AAAACCCCCGGCAATAACAA	151	**BG934348**
	R	CTAGGACCTGAAAGCAGCACG		
Segm 5	F	GGAAAGCCCTGCTCTGGC	51	**AY853932**
	R	TCCTCAAGTCTGCTTCGGGA		

Table 5.1: Real-Time PCR primers designed and used in the present study. The different primer sets are noted a and b. There are all together four primer set for two cIAP-1 genes (to separate them one is marked with "(1)") due to changes in the Genebank late in this study.

Genes	Dir.	Sequence	Amp.	E-value	Acc.no
MX	F	TGATCGATAAAGTGACTGCATTCA	80	0,99	**SSU66477**
	R	TGAGACGAACTCCGCTTTTTCA			
INF-α	F	CCTGCCATGAAACCTGAGAAGA	107	0,96	**AY216594**
	R	TTTCCTGATGAGCTCCCATGC			
18S	F	TGTGCCGCTAGAGGTGAAATT	61	1,00	**AJ427629**
	R	GCAAATGCTTTCGCTTTCG			
EF1 α	F	CACCACCGGCCATCTGATCTACAA	77	0,97	**AF321836**
	R	TCAGCAGCCTCCTTCTCGAACTTC			

Table 5.2: Real-Time PCR primers used in the present study. (Already designed and tested by S.M. Jørgensen (Jorgensen, Kleveland et al. 2006)). Dir = direction; Amp = amplicon size; E-value = primer efficiency and Acc.no = Accession number.

6. METHODES

6.1 Cell cultures

ASK cells (Atlantic salmon kidney cells), kindly provided by B. Krossøy (Department of Fisheries and Marine Biology, University of Bergen, Norway) were cultured in Leibovitz L-15 medium (Cambrex Bio Sciences, Verviers, Belgium) supplemented with 50 μg μl^{-1} gentamicin, 4 mM L-glutamine, 40 μM β-mercaptoethanol and 10% foetal bovine serum (L-15 complete). The SHK-1 cell line (Salmon head kidney), kindly provided by B. Dannevig (National Veterinary Institute, Oslo, Norway), were also cultured in Leibovitz L-15, but with 5% foetal bovine serum. Cells were routinely split 1:3 once a week and maintained at 20 ºC.

6.2 Virus production

Inoculation of ISAV (strain Glesvaer/2/90 was kindly provided by B. Dannevig, with a virus titer of $1\times10^{5.7}$ $TCID_{50}$ ml^{-1}, which had been passaged two times in SHK-1 cells and stored at -80 ºC until use, was performed on SHK-1 cells grown in 500 cm^2 cell culture flasks. The cell culture medium was removed, and the cells were washed twice in phosphate buffered saline (PBS) pH 7,4, before 20 ml ISAV inoculate, diluted 1:50 in serum-free medium, was added. The virus was allowed to adsorb for 4 h at 15 ºC, followed by the addition of 100 ml L-15 complete medium. Infection was allowed to proceed at 15 ºC for 20 days to ensure enough virus replication.

Cell culture supernatant from ISAV-infected SHK-1 cells was cleared from cell debris by low speed centrifugation at 4000 x g for 20 min at 4 ºC (Beckman Avanti J-25 centrifuge with JA-10 rotor was used).

To further separate virus from remaining serum proteins, 4 ml 20% sucrose solution was applied, using a syringe (Terumo), in the bottom of six polyallomer tubes (supplied by Beckman), and 32 ml of the cell culture supernatant was gently poured on top of it (important to make sure the two layers don't mix together). The tubes containing supernatant and sucrose solution were then centrifuged at 104000 x g for 2 h at 4 ºC (Sorvall Discovery 100 centrifuge

with Surespin 630 rotor). The supernatant and sucrose were then discarded. The sucrose step was repeated so all virus was pelleted and filtered through the sucrose solution.

The six tubes containing the virus pellets were then washed two times with PBS to remove remaining medium and sucrose. Furthermore, 2 ml of PBS pH 7,4 was applied to one tube and a sonicator rod (Vibra Cell, Sonic & Materials inc., Danbury, CT, USA) was used, three times for 2 sec, to resuspend the pelleted virus in the PBS solution. The PBS solution containing the ISA virus was then moved from tube to tube, with disruption of the pelleted virus in every tube. The final 2 ml PBS solution containing all the virus from all six tubes, was then divided into 200 µl samples and stored at -80 ºC until use.

6.3 Infection of ASK and SHK cells

SHK and ASK cells were seeded in six-well tissue-culture plates (culture area, 9,6 cm^2/well)(Nunc, Roskilde, Denmark). The cells were counted and $1,5 \times 10^5$ cells were seeded with 3 ml L-15 complete medium in each well ($1,5 \times 10^4$ cells/cm^2). The cells were then grown for 48 h at 20 ºC before infection with ISA virus.

After 48 h, the medium from each well was collected of and kept for later use, before the wells were washed three times with PBS pH 7,4. Then 600 µl ISAV inoculate (MOI = 0,025), diluted 1:50 in serum-free medium, was added and the plates were inoculated on a rock tray "The Belly Button" (Stovall Life Science Greenboro, NC, USA) for 4 h at 15 ºC. The control-wells were mock-infected with 600 µl serum-free medium instead of ISAV inoculate.

After inoculation the stored medium was diluted 50:50 with serum-free medium and 2,4 ml was added to the wells. The dishes were then sealed with PCR Adhesive Sealing Sheets (Eppendorf, Hamburg, Germany) and stored at 15 ºC until harvest.

Cells were harvested at 1, 3, 5, 7 and 9 days post infection (p.i) by collecting the cell medium in a 15 ml collection tube, before scraping the cell monolayer in 2 ml PBS three times to ensure that all infected cells are loosened and collected in the collection tube.
The tube, containing cells suspended in PBS and medium, was then pelleted at 300 x g for 10 min (Sorvall RC 3C Pluss). To ensure complete removal of the cell culture medium, which can inhibit lysis of the cells by Buffer RTL, everything but the cell-pellet were removed and

10 ml of PBS pH 7,4 was added. Another centrifugation at 300 x g for 10 min was then done before the PBS was discarded.

The washed cell-pellet was then lysed and homogenized according to manufacturer's guidelines (RNeasy® Mini Kit) and stored at -80 ºC until further RNA extraction.

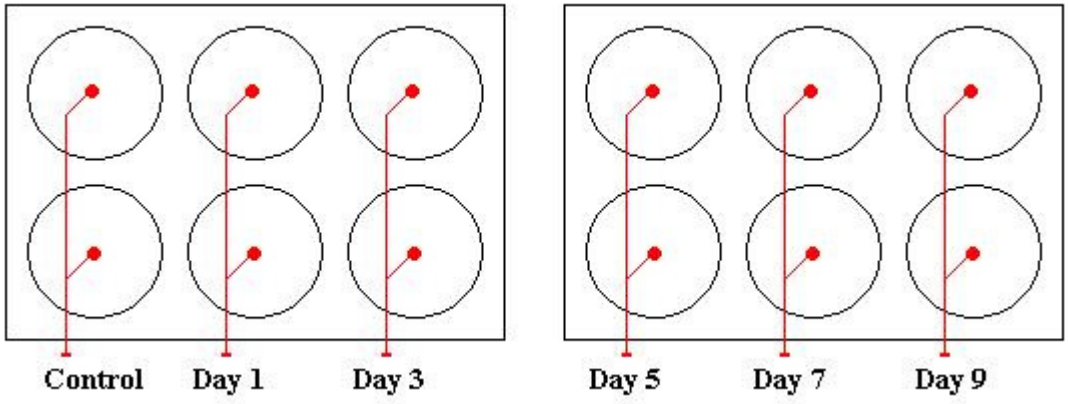

Figure 6.1: Six-well tissue culture plate setup for ASK and SHK infections.

The plate setup seen above was used for both ASK and SHK. Two wells were pooled for each day to ensure enough cell material and a high RNA yield for further use in total RNA isolation.

6.4 Treatment of ASK and SHK cells with Staurosporine.

SHK and ASK cells were seeded in six-well tissue-culture plates (culture area, 9,6 cm^2/well). The cells were counted and $1,0 \times 10^6$ cells were seeded with 3 ml L-15 complete medium in each well ($1,0 \times 10^5$ cells/cm^2).

The cells were then grown for 24 h at 20 ºC, before 3 µl staurosporine (SS) solution (1mM) was added to four of the wells for both SHK and ASK. Two wells were added 3 µl DMSO, which is used as a solvent in the staurosporine-solution, and were used as control samples. Cells were harvested 24 h and 48 h, after addition of staurosporine, as described above in section 6.3. And the cells where then stored at -80 ºC until use.

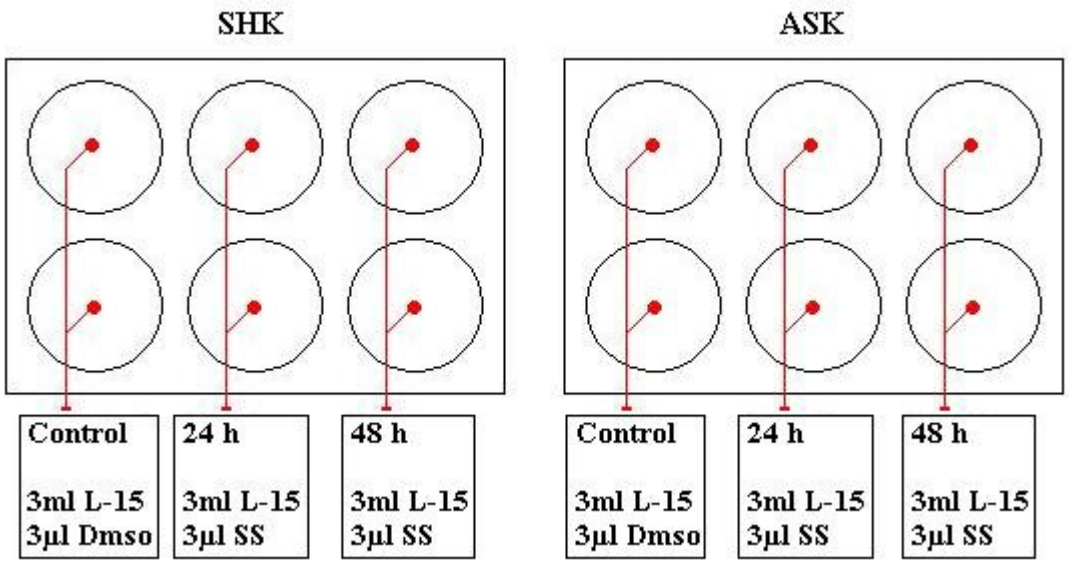

Figure 6.2: Six-well tissue culture plate setup for Staurosporine treatment of ASK and SHK. Two wells were used for each day to ensure enough cell material and a high RNA yield for further use in total RNA isolation.

6.5 RNA extraction

Total RNA was isolated from treated cells using RNeasy® Mini Kit (Qiagen, MD, USA) according to manufacturer's instructions. Because the RNA was to be used further in RT TaqMan analysis and Real-time PCR which is sensitive to very small amounts of non-target DNA, the on-column RNase free DNase set (Qiagen, MD, USA) was also used according to manufacturer's instructions to ensure digestion and removal of small residual amounts of DNA in the column.

Total RNA was eluted in a final volume of 40 µl RNase-free water (Eppendorf, Hamburg, Germany). The quality and quantity of the purified nucleic acids were determined by measuring the optical density (OD) at 260 nm/280 nm (OD_{260}/OD_{280}). OD values were measured with the RNA-program in Beckman DU®530 Spectrophotometer, using 2 µl RNA-solution diluted in 98 µl RNase-free water for each sample measurement. The RNA-solutions were then stored immediately at -80 ºC until RT-PCR

6.6 cDNA synthesis

All samples were reverse transcribed using TaqMan® Reverse Transcription reagents (Applied Biosystems, CA, USA) according to manufacturer's protocol and with random hexamer primers. For every sample, 2 µg of total RNA was transcribed in a 100 µl reaction. The amount of RNA-solution needed for the reaction was calculated by using this equation:

$$\text{Amount of RNA-solution used} = \frac{2000}{\mu g/ml} = x\ \mu l$$

PCR reaction in each tube (total volume of 100 µl) also consists of:

10 µl	10x RT Buffer
22 µl	$MgCl_2$ Solution
20 µl	dNTP Mix (with dTTP)
5 µl	Random Hexamers
2 µl	RNase Inhibitor
2,5 µl	Reverse Transcriptase
38,5 µl – amount of RNA-solution used	RNase-free water

All samples were reverse transcribed in Eppendorf Mastercycler gradient, using the already made program called SMRT18. (1st cycle: annealing at 25 °C for 10 minutes, 2nd cycle: polymerisation at 37 ºC for 60 minutes, 3rd cycle: denaturation at 95 ºC for 5 minutes and last 4th cycle: cooling at 4 ºC for up to 60 minutes.)

6.7 Real-time PCR

For each infection trial, real-time PCR was performed in 96-well optical plates on an ABI Prism 7000 Sequence Detection system (Applied Biosystems). In each well reactions were conducted in a final volume of 25 µl containing 12,5 µl SYBR® GREEN PCR Master Mix, 5,5 µl Molecular Biology Grade Water, 1 µl forward primer, 1 µl reverse primer and 5 µl cDNA diluted 1:10, except for a 1:1000 dilution of the cDNA used with the 18S-primers. Controls were conducted for each primer set, using 5 µl Molecular Biology Grade Water instead of cDNA. Each reaction was done with two parallel's (same reaction in two wells) to ensure that both samples showed the same results, and that no unwanted contamination had interfered with the reaction in any of the wells.
18S and EF1α, which are considered as valid housekeeping genes and are relative stable during infection, were used as reference genes (Jorgensen, Kleveland et al. 2006).
Primers for ISAV segment 5 were also used to verify that the cells were infected properly.

PCR parameters were 50 ºC for 2 min, 95 ºC for 10 min, followed by 40 cycles of 95 ºC for 15 s, 60 ºC for 1 min.

	1	2	3	4	5	6	7	8	9	10	11	12
A	**18S** Bl	**EF1α** Bl	**IFNα** Bl	**MX** Bl	**P53** Bl	**Segm5** Bl	**cIAP** Bl	**Pdcd5** Bl	**Bcl2l** Bl	**cIAP(2)** Bl	**Casp3** Bl	
B	**18S** Bl	**EF1α** Bl	**IFNα** Bl	**MX** Bl	**P53** Bl	**Segm5** Bl	**cIAP** Bl	**Pdcd5** Bl	**Bcl2l** Bl	**cIAP(2)** Bl	**Casp3** Bl	
C	**18S** Ctrl *10^{-3}*	**EF1α** Ctrl *10^{-1}*	**IFNα** Ctrl *10^{-1}*	**MX** Ctrl *10^{-1}*	**P53** Ctrl *10^{-1}*	**Segm5** Ctrl *10^{-1}*	**cIAP** Ctrl *10^{-1}*	**Pdcd5** Ctrl *10^{-1}*	**Bcl2l** Ctrl *10^{-1}*	**cIAP(2)** Ctrl *10^{-1}*	**Casp3** Ctrl *10^{-1}*	
D	**18S** Ctrl *10^{-3}*	**EF1α** Ctrl *10^{-1}*	**IFNα** Ctrl *10^{-1}*	**MX** Ctrl *10^{-1}*	**P53** Ctrl *10^{-1}*	**Segm5** Ctrl *10^{-1}*	**cIAP** Ctrl *10^{-1}*	**Pdcd5** Ctrl *10^{-1}*	**Bcl2l** Ctrl *10^{-1}*	**cIAP(2)** Ctrl *10^{-1}*	**Casp3** Ctrl *10^{-1}*	
E	**18S** D 1 *10^{-3}*	**EF1α** D 1 *10^{-1}*	**IFNα** D 1 *10^{-1}*	**MX** D 1 *10^{-1}*	**P53** D 1 *10^{-1}*	**Segm5** D 1 *10^{-1}*	**cIAP** D 1 *10^{-1}*	**Pdcd5** D 1 *10^{-1}*	**Bcl2l** D 1 *10^{-1}*	**cIAP(2)** D 1 *10^{-1}*	**Casp3** D 1 *10^{-1}*	
F	**18S** D 1 *10^{-3}*	**EF1α** D 1 *10^{-1}*	**IFNα** D 1 *10^{-1}*	**MX** D 1 *10^{-1}*	**P53** D 1 *10^{-1}*	**Segm5** D 1 *10^{-1}*	**cIAP** D 1 *10^{-1}*	**Pdcd5** D 1 *10^{-1}*	**Bcl2l** D 1 *10^{-1}*	**cIAP(2)** D 1 *10^{-1}*	**Casp3** D 1 *10^{-1}*	
G	**18S** D 3 *10^{-3}*	**EF1α** D 3 *10^{-1}*	**IFNα** D 3 *10^{-1}*	**MX** D 3 *10^{-1}*	**P53** D 3 *10^{-1}*	**Segm5** D 3 *10^{-1}*	**cIAP** D 3 *10^{-1}*	**Pdcd5** D 3 *10^{-1}*	**Bcl2l** D 3 *10^{-1}*	**cIAP(2)** D 3 *10^{-1}*	**Casp3** D 3 *10^{-1}*	
H	**18S** D 3 *10^{-3}*	**EF1α** D 3 *10^{-1}*	**IFNα** D 3 *10^{-1}*	**MX** D 3 *10^{-1}*	**P53** D 3 *10^{-1}*	**Segm5** D 3 *10^{-1}*	**cIAP** D 3 *10^{-1}*	**Pdcd5** D 3 *10^{-1}*	**Bcl2l** D 3 *10^{-1}*	**cIAP(2)** D 3 *10^{-1}*	**Casp3** D 3 *10^{-1}*	

	1	2	3	4	5	6	7	8	9	10	11	12
A	**18S** D 5 *10^{-3}*	**EF1α** D 5 *10^{-1}*	**IFNα** D 5 *10^{-1}*	**MX** D 5 *10^{-1}*	**P53** D 5 *10^{-1}*	**Segm5** D 5 *10^{-1}*	**cIAP** D 5 *10^{-1}*	**Pdcd5** D 5 *10^{-1}*	**Bcl2l** D 5 *10^{-1}*	**cIAP(2)** D 5 *10^{-1}*	**Casp3** D 5 *10^{-1}*	
B	**18S** D 5 *10^{-3}*	**EF1α** D 5 *10^{-1}*	**IFNα** D 5 *10^{-1}*	**MX** D 5 *10^{-1}*	**P53** D 5 *10^{-1}*	**Segm5** D 5 *10^{-1}*	**cIAP** D 5 *10^{-1}*	**Pdcd5** D 5 *10^{-1}*	**Bcl2l** D 5 *10^{-1}*	**cIAP(2)** D 5 *10^{-1}*	**Casp3** D 5 *10^{-1}*	
C	**18S** D 7 *10^{-3}*	**EF1α** D 7 *10^{-1}*	**IFNα** D 7 *10^{-1}*	**MX** D 7 *10^{-1}*	**P53** D 7 *10^{-1}*	**Segm5** D 7 *10^{-1}*	**cIAP** D 7 *10^{-1}*	**Pdcd5** D 7 *10^{-1}*	**Bcl2l** D 7 *10^{-1}*	**cIAP(2)** D 7 *10^{-1}*	**Casp3** D 7 *10^{-1}*	
D	**18S** D 7 *10^{-3}*	**EF1α** D 7 *10^{-1}*	**IFNα** D 7 *10^{-1}*	**MX** D 7 *10^{-1}*	**P53** D 7 *10^{-1}*	**Segm5** D 7 *10^{-1}*	**cIAP** D 7 *10^{-1}*	**Pdcd5** D 7 *10^{-1}*	**Bcl2l** D 7 *10^{-1}*	**cIAP(2)** D 7 *10^{-1}*	**Casp3** D 7 *10^{-1}*	
E	**18S** D 9 *10^{-3}*	**EF1α** D 9 *10^{-1}*	**IFNα** D 9 *10^{-1}*	**MX** D 9 *10^{-1}*	**P53** D 9 *10^{-1}*	**Segm5** D 9 *10^{-1}*	**cIAP** D 9 *10^{-1}*	**Pdcd5** D 9 *10^{-1}*	**Bcl2l** D 9 *10^{-1}*	**cIAP(2)** D 9 *10^{-1}*	**Casp3** D 9 *10^{-1}*	
F	**18S** D 9 *10^{-3}*	**EF1α** D 9 *10^{-1}*	**IFNα** D 9 *10^{-1}*	**MX** D 9 *10^{-1}*	**P53** D 9 *10^{-1}*	**Segm5** D 9 *10^{-1}*	**cIAP** D 9 *10^{-1}*	**Pdcd5** D 9 *10^{-1}*	**Bcl2l** D 9 *10^{-1}*	**cIAP(2)** D 9 *10^{-1}*	**Casp3** D 9 *10^{-1}*	
G												
H												

Table 6.1: Example of Real-Time PCR plate setup for one infection trial.

Primers displayed in **bold**, cDNA dilution showed in *italic* and the number of days the cells were harvested post infection (p.i) displayed in the middle. (D 1 = 1 day p.i, D 3 = 3 days p.i, etc).

6.8 Primer Design

The genes used as the base for primer design were found at The Gene Index Project (http://compbio.dfci.harvard.edu/tgi/), by searching the Atlantic salmon (*Salmon salar*), Catfish (*Ictalurus punctatus*) and Zebrafish (*Danio rerio*) gene indices for genes related to apoptosis. Genes of interest were then compared to ESTs (Expressed Sequence Tags) from the Atlantic salmon gene bank, using Blastn (http://compbio.dfci.harvard.edu/tgi/cgi-bin/tgi/Blast/index.cgi)

Real-time PCR primers (Table 5.1) were then designed manually based on Primer Express 2.0 software guidelines (Applied Biosystems) and synthesised by either Invitrogen (CA, USA) or ProOligo (Paris, France). For each gene, 2 different primers were designed and synthesised to ensure that at least one of them worked satisfactory. Other primers used in this study, had already been designed and tested by Jørgensen S.M (Jorgensen, Kleveland et al. 2006)(Table 5.2).

6.9 Primer efficiency tests

Primer efficiency of the new primers was tested, using real-time PCR carried out with 10-fold dilutions of cDNA. Controls (no cDNA) and 1:1, $1:10^1$, $1:10^2$ and $1:10^3$ dilutions were used for each primer set. Ct- values from the results were then exported to Sigmaplot 8.0 and linear regression graphs were made by plotting Ct-values on the y-axis and log concentrations of the cDNA on the x-axis.

R^2 was then calculated to see how well the linear relationship between Ct values and log concentrations corresponded. The slope of the graph was then calculated and amplification efficiency of the reactions was then calculated using the following formula: (Rasmussen 2001)

$$\text{Exponential amplification} = 10^{(-1/\text{slope})}$$

$$\text{Efficiency} = [10^{(-1/\text{slope})}] - 1$$

Where maximal efficiency (1) means that every single template is replicated in each cycle.

All primers were also tested for the possibility of primer dimers and unspecific products, by analyzing melting curves for the real-time PCR reactions for every primer set.

6.10 Primer amplification products tests

The real-time PCR products were tested by agarose gel electrophoresis, by comparing theoretical amplicon size (table 5.1) to obtained fragment size. Agarose gel electrophoresis was done with the FlashGel^{TM} System Kit, delivered by Cambrex Bio Science Rockland, ME, USA.

Each sample well was loaded with 7 µl deionized water. One well was then added 5 µl FlashGel^{TM} DNA Marker (band sizes: 100 / 200 / 300 / 500 / 800 / 1250 / 2000 / 4000 bp) and the wells for the samples were added a mix of 1 µl DNA solution and 4 µl FlashGel^{TM} Loading Dye. The power supply was then set to 150 V constant voltages, and the gel was run until desired separation was obtained.

The fragments on the FlashGel^{TM} Cassette were then illuminated by UV-light using BioRad Gel Doc 1000 Darkroom. The results were then viewed and pictures were taken with Multi-Analyst Version 1.1.

6.11 Real-time PCR data analysis

Data handling was done according to the ABI Prism 7000 Sequence Detection System User Manual and baseline and cycle threshold (C_t) were set automatically by ABI Prism 7000 System Software for each PCR-reaction. High Ct-values (Ct > 35) were discarded manually, as were reactions with low fluorescence compared to the background fluorescence (fluorescence < 4000).

To calculate the relative expression of the target genes, Ct-values for target genes and reference genes were analyzed using the Relative Expression Software Tool (REST©) (Pfaffl, Horgan et al. 2002). Results from REST were then exported to Excel and relative expression graphs were made of the target genes for each infection trial over time.

7. RESULTS

7.1 Primer Tests

Note that the cIAP-1 gene has two different primer sets, and therefore have been analyzed twice in this study. Late in this study the tentative consensus with accession number tc29339, was spilt into two new tentative consensus sequences with accession number tc57717 and tc43301. By aligning the old sequence with the two new sequences, using bl2seq (http://www.ncbi.nlm.nih.gov/blast/bl2seq/wblast2.cgi), and comparing this to the starting point for the primers (obtained from Primer Express 2.0), we discovered that the primer set for tc29339 was located on the new tc43301 sequence which is highly similar (92% hit coverage) to the cIAP-1 gene in Catfish.

7.1.1 Primer efficiency testing

The efficiency of a PCR reaction can be deducted by the slope of a standard curve according to equation: Efficiency = $[10^{(-1/slope)}] - 1$ (Rasmussen 2001)
The maximum efficiency in PCR is 1, where every PCR product is replicated in every cycle. The minimum value is 0, corresponding to no amplification.

To calculate primer efficiency, real-time PCR were done with cDNA obtained from untreated SHK cells. For each primer-set, a control (no cDNA) and 10-fold dilutions of cDNA ranging from 1:1 to $1:10^{-3}$ were used. Figure 7.1 shows an amplification plot of the PCR reactions for the cIAP-1a primers set. Amplification plots for the other primer set are not shown.

Figure 7.1: Real-time amplification plot of 10 fold serial dilutions. 7000 System SDS Software Amplification plot for the cIAP-1a primer set, with cDNA dilutions ranging from 1:1 to $1:10^{-3}$. Note that the dilution containing the highest cDNA concentration exhibits fluorescence earlier than the one with the second highest concentration and so on.

High Ct-values (Ct > 35) were discarded manually, and the results were exported to Sigmaplot 8.0. Linear regression graphs for each primer set are displayed below (Figure 7.2 a-f).

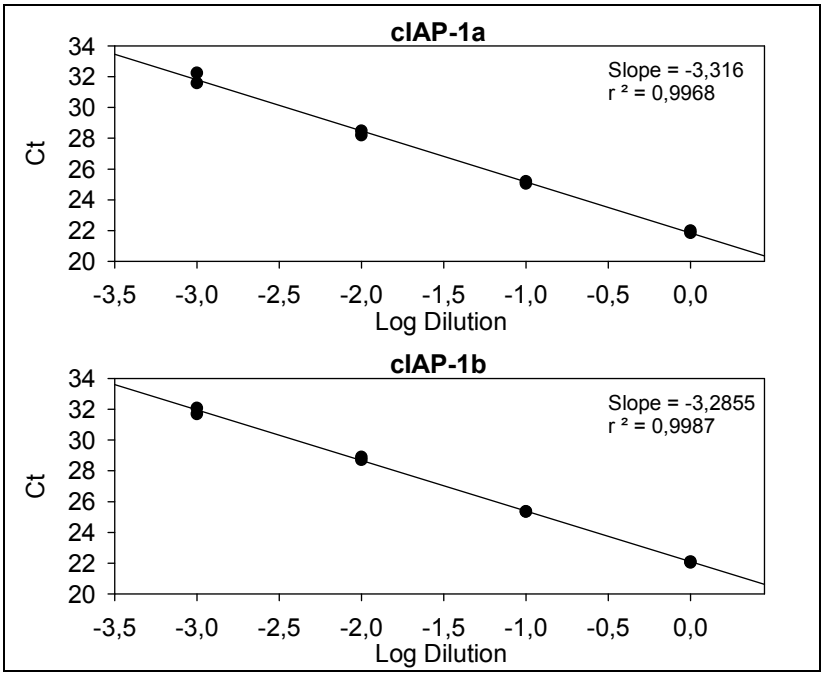

Figure 7.2 a: Linear regression plots for cIAP-1. The two different primer sets are noted *a* and *b*. The graphs show the relationship between Ct-values and log-concentrations.

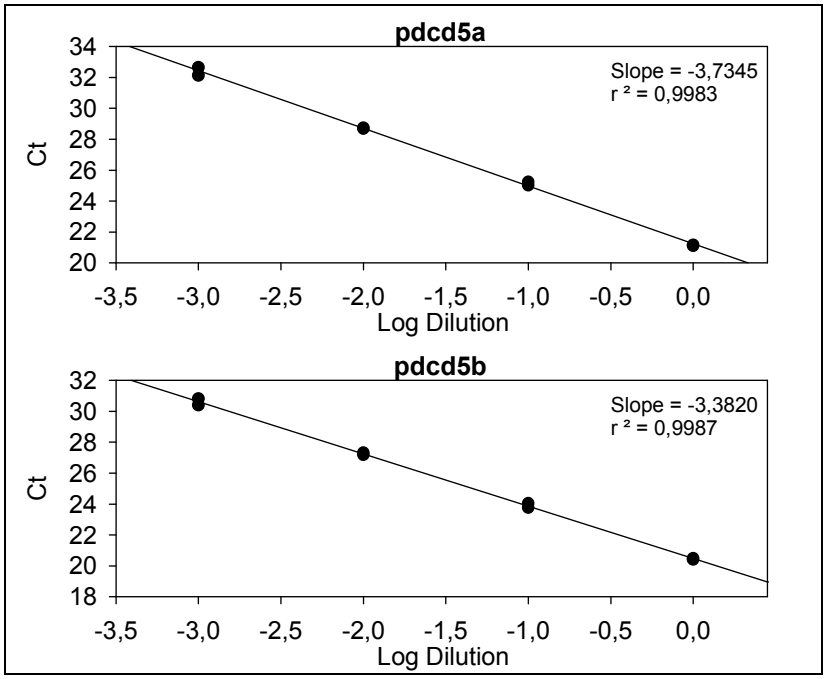

Figure 7.2 b: Linear regression plots for pdcd5. The two different primer sets are noted *a* and *b*. The graphs show the relationship between Ct-values and log-concentrations.

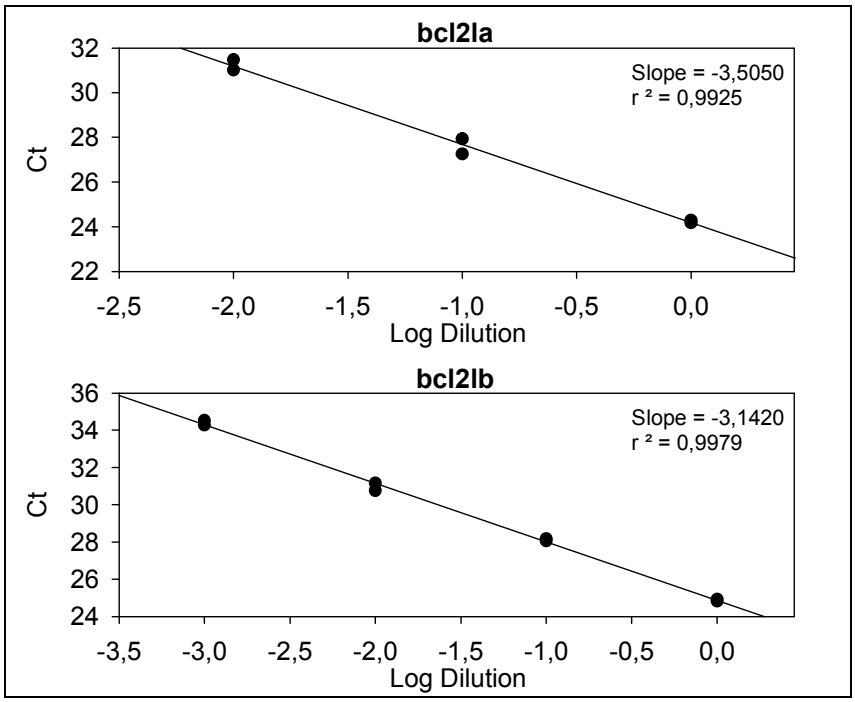

Figure 7.2 c: Linear regression plots for bcl2l. The two different primer sets are noted *a* and *b*. The graphs show the relationship between Ct-values and log-concentrations.

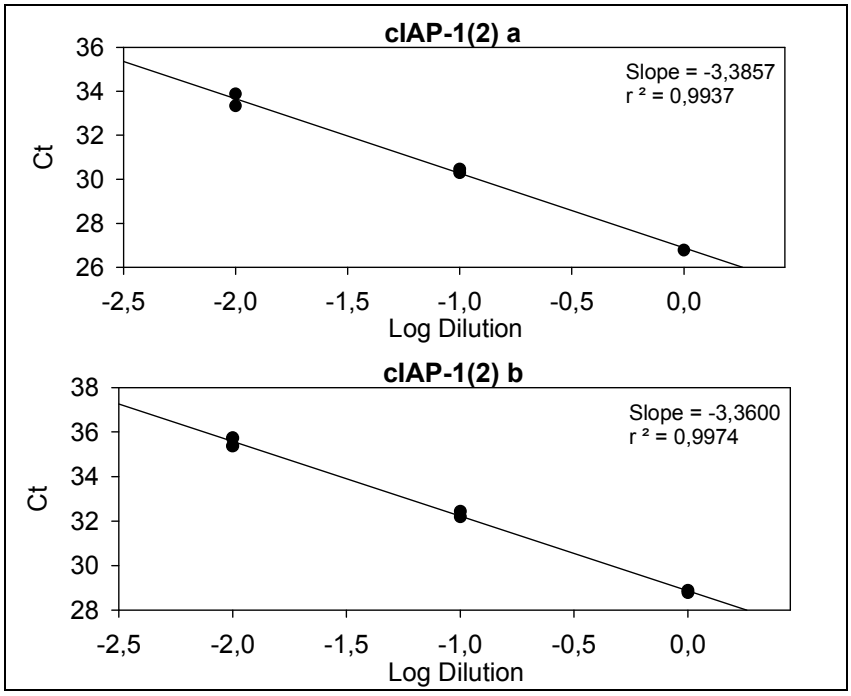

Figure 7.2 d: Linear regression plots for cIAP-1(2). The two different primer sets are noted *a* and *b*. The graphs show the relationship between Ct-values and log-concentrations.

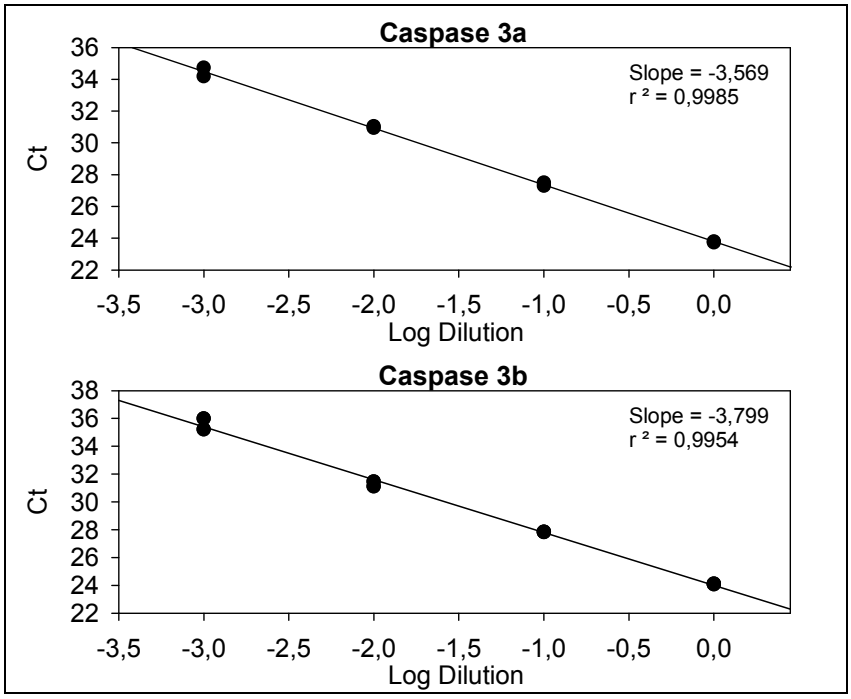

Figure 7.2 e: Linear regression plots for Caspase 3. The two different primer sets are noted *a* and *b*. The graphs show the relationship between Ct-values and log-concentrations.

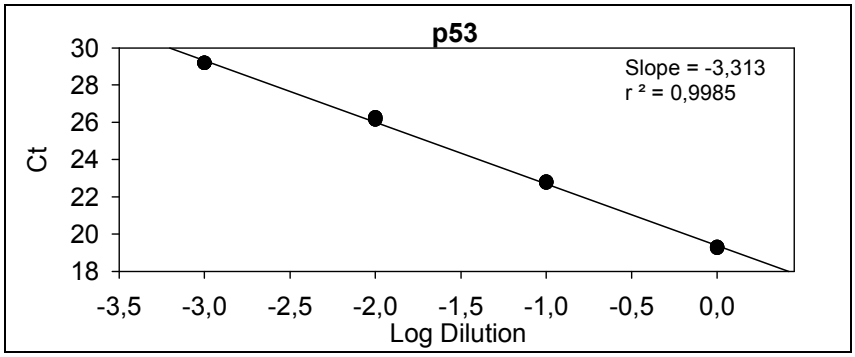

Figure 7.2 f: Linear regression plot for p 53. The graph shows the relationship between Ct-values and log-concentrations.

For each reaction series, there was high correlation between cycle number and dilution factor ($r^2 = 1 \pm 0{,}005$), and for each gene there was at least one primer set with a slope value close to the optimum theoretical value of -3,32 (Snow, McKay et al. 2006).
The slope value for each primer set was then used in the efficiency-equation, and results are displayed in Table 7.1.

Primer set	Slope	E-value
cIAP-1 a	-3,32	1,00
cIAP-1 b	-3,29	1,01
pdcd5 a	-3,73	0,85
pdcd5 b	-3,38	0,98
bcl2l a	-3,51	0,93
bcl2l b	-3,14	1,08
cIAP-1(2) a	-3,39	0,97
cIAP-1(2) b	-3,36	0,98
Caspase 3 a	-3,57	0,91
Caspase 3 b	-3,80	0,83
p53	-3,31	1,00

Table 7.1: Efficiency values calculated for the primers used in present study.

7.1.2 Melting curve analysis (elimination of primer dimers)

DNA binding dyes, such as SYBR Green, detect all dsDNA including primer dimers and other undesired products. The specificity of detection is therefore dependent on the specificity of the amplification. However this problem can be solved by analyzing the melting curves of the PCR reaction.

Plotting fluorescence as a function of temperature as the thermal cycler heats through the dissociation temperature of the product gives a DNA melting curve. The shape and position of this DNA melting curve are functions of the GC/AT ratio, length, and sequence and can be used to differentiate amplification products separated by less than 2 ºC in melting temperature (Ririe, Rasmussen et al. 1997).

The melting curve of the cIAP-1a PCR products is shown in figure 7.3. Melting curves were analyzed for every primer set, and indicated a single melting peak similar to the one in figure 7.3, suggesting that amplification products were specific (data not shown).

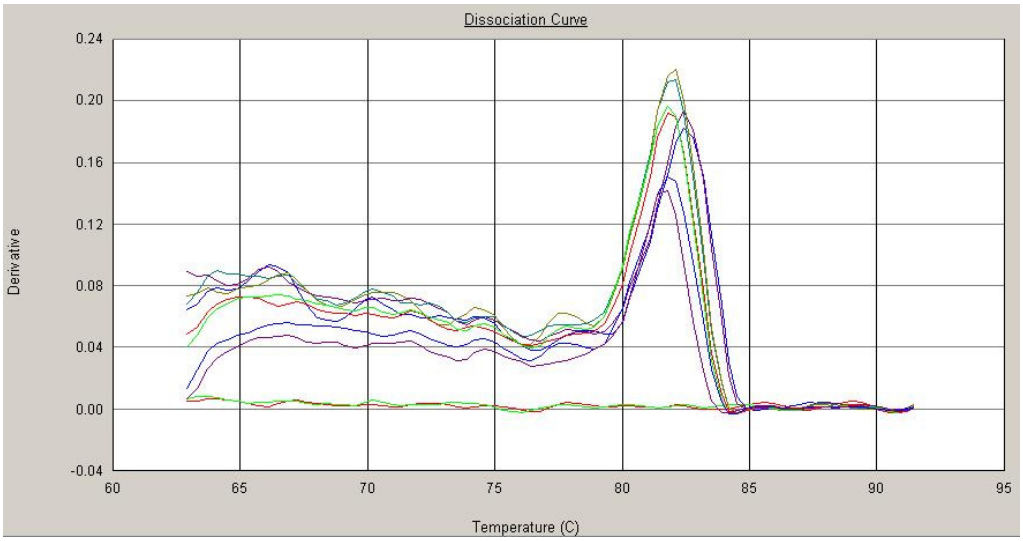

Figure 7.3: Melting peak of cIAP-1a PCR products. A single melting peak (T_m) at approximately 82 ºC, indicating that the amplification was gene-specific. X-axis displays temperature and Y-axis (derivate) displays change in fluorescence (-dF/dT).

Based on the results from both efficiency testing and melting curve analysis, the best primers for each gene were picked out for further use in the infection and Staurosporine trials.

The primers selected for further use were:

- cIAP-1 a
- pdcd5 b
- bcl2l a
- cIAP-1(2) b
- Caspase 3 b
- p53

Both caspase 3a and b primers were used in the first infection trials, but the PCR-reactions with the caspase 3a primer resulted in very high C_t-values (above 35). This was probably due to personal errors (e.g. pipetting errors when loading the 96-well plate). To be able to compare results from different infection trial, the Caspase 3b primer set, which resulted in better C_t-values in the infection trials, was chosen for further use.

7.1.3 Gel electrophoresis of amplicons

As described in (Lekanne Deprez, Fijnvandraat et al. 2002), PCR amplification products should also be tested by agarose gel electrophoresis to ensure primer specificity. All amplicons were run on an agarose gel, and the obtained fragment sizes corresponded to the theoretical amplicon sizes displayed in Table 5.1. Gel electrophoresis results are shown in Figure 7.4.

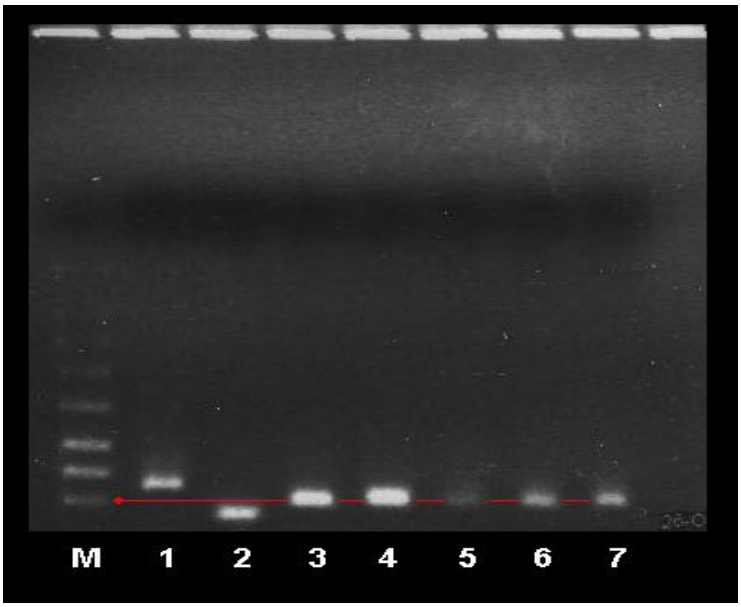

Figure 7.4: Gel electrophoresis of the real-time PCR products of the primers. Lane M contains FlashGel™ DNA Marker (band sizes: 100/200/300/500/800/1250/2000/4000 bp). Lanes 1-7 represent amplification products from p53, Segm5, cIAP-1a, pdcd5b, bcl2la, cIAP-1(2) b and Caspase3b, respectively. The 100 bp band is marked with a red line. The agarose gel was visualized under UV-light and picture was taken with Multi-Analyst Version 1.1.

7.2 Gene expression in ASK and SHK cells after treatment with staurosporine

Both ASK and SHK cells were treated with staurosporine as described in section 6.4. Staurosporine caused a rapid development of cytopathic effect (CPE) in both cell lines. After the first 24 hours, the cells had already "shrinked" from a flattened morphology, to a more rounded up structure. Many of the cells had also detached from the cell-monolayer. After 48 hours of SS treatment almost all of the cells had detached from the cell-monolayer.

All reactions for both SHK and ASK treated with staurosporine, showed high fluorescence, good parallels and low Ct-values. None were discarded. The graphs made in excel based on relative expression levels calculated in REST are displayed below:

7.2.1 SHK cells treated with staurosporine

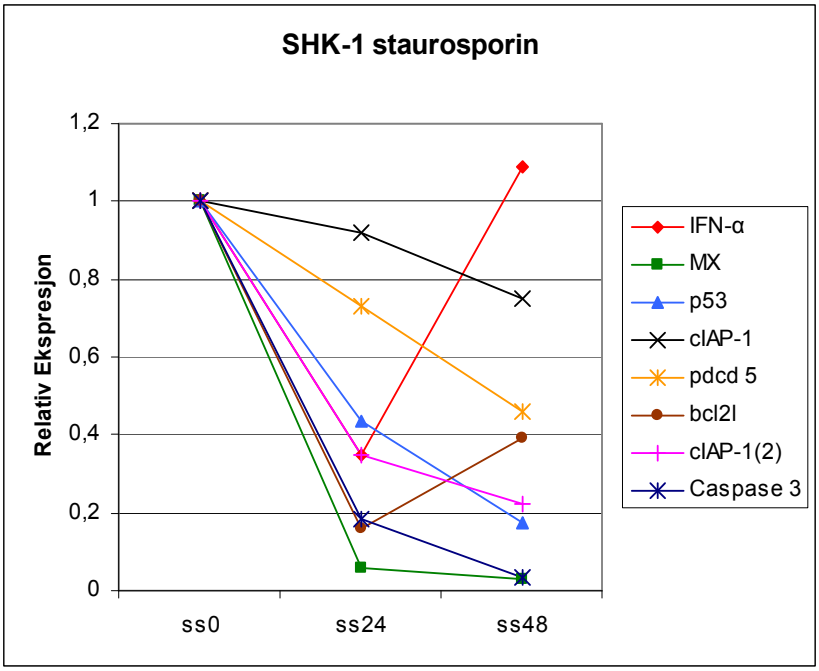

Figure 7.5: Relative expression of INF α, MX, p 53, cIAP-1, pdcd 5, Bcl2l, cIAP-1(2) and Caspase 3.

7.2.2 ASK cells treated with staurosporine

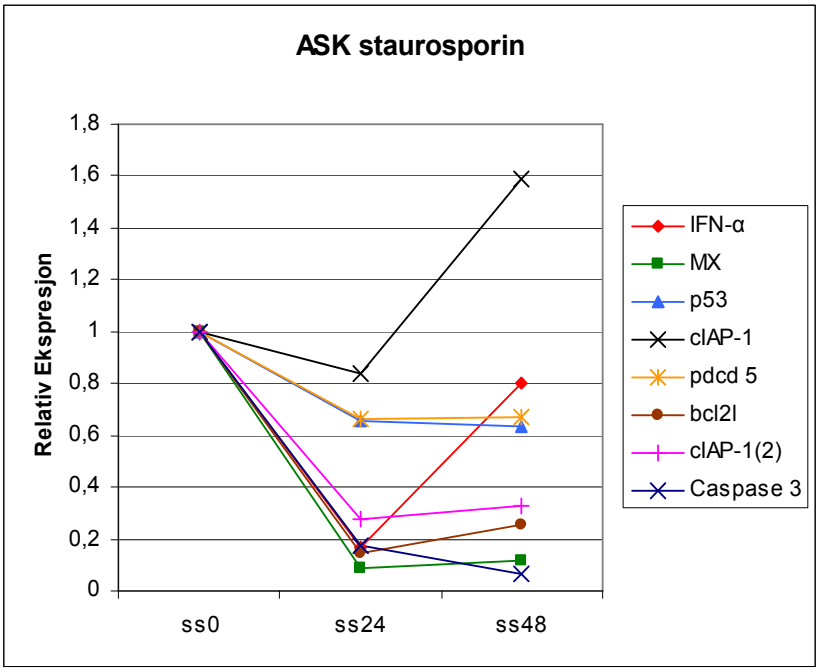

Figure 7.6: Relative expression of INF α, MX, p 53, cIAP-1, pdcd 5, Bcl2l, cIAP-1(2) and Caspase 3.

Summary of results from cells treated with staurosporine

Staurosporine is a general inhibitor of many protein kinases, including protein kinase C, A and G, and is commonly used to induce apoptosis in cell-cultures (Mannherz, Gonsior et al. 2006). We wanted to compare changes in gene expression from cells infected with ISAV to cells treated with staurosporine, to see if the changes observed in the ISAV infected cells were a result of the ILA virus infection and not just a general change due to the apoptosis.

Unfortunately, the cells treated with staurosporine did not show any significant regulation of any genes of interest and will therefore not be comparable to the ISAV infected cells. In previous staurosporine experiments done earlier in this study, we had some problems with extracting enough RNA for cDNA synthesis from the treated cells (data not shown). This, together with the relative expression results, indicates that staurosporine, used in concentrations of 1µM, might be toxic to both ASK and SHK cells, leaving the cells no time to regulate their gene expression. A lower concentration of staurosporine might therefore be preferable in future studies with staurosporine treatment of ASK and SHK cells.

7.3 Viral replication

To monitor viral replication by means of increased viral mRNA levels of ISAV segment 5 (encoding a membrane fusion protein called gp50), real-time PCR was performed on cDNA synthesized from total RNA samples of SHK and ASK cells at 1, 3, 5, 7 and 9 days post infection. Figure 7.7 shows relative expression levels of segment 5 in SHK cells (infection trial 3 and 4 in section 7.4.1) calculated relative to day 1 post infection.

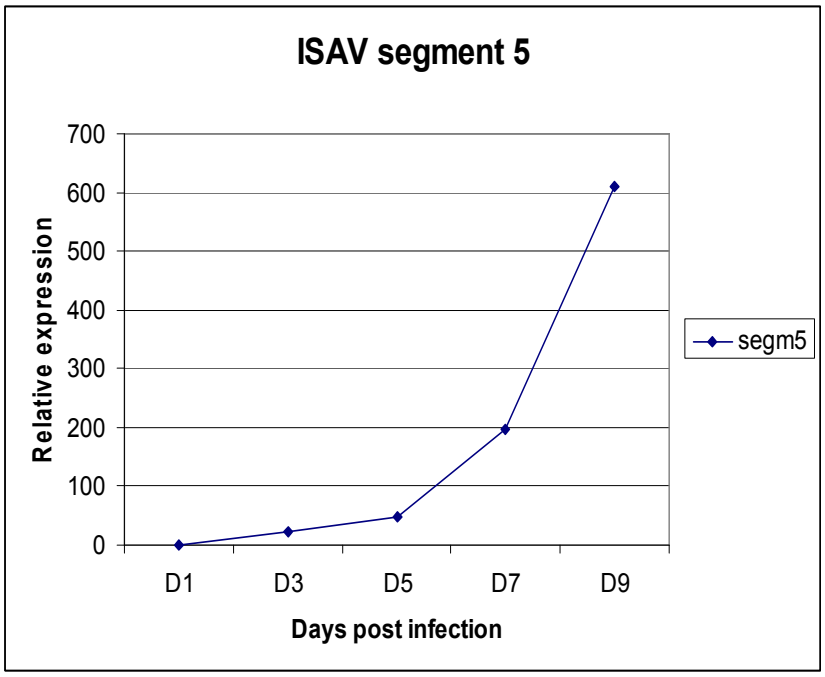

Figure 7.7: Relative mRNA transcription of ISAV segment 5 at 1, 3, 5, 7, and 9 days p.i. Relative transcription levels are calculated in REST for D3-D9. Relative expression of day 1, which all other days are calculated relative against, are manually set to 1.

As figure 7.7 shows, transcription of ISAV segment 5 increased steadily throughout the infection, indicating an increasing viral replication in SHK cells after infection. Transcription of Segment 5 was also analyzed on ASK cells and showed similar results of increasing viral replication during infection (data not shown). Increasing viral replication in ASK cells have also been observed in other studies (Jorgensen, Lyng-Syvertsen et al. 2006).

7.4 Gene expression in ASK and SHK cells after ISAV infection

Both SHK and ASK cells were infected with ISAV as described in section 6.3. Note that in infection trials 1 and 2 for SHK and trial 1 for ASK, samples were not taken at day 1 post infection.

ISA virus infected and replicated in both SHK and ASK cells, and caused acute infections and development of cytopathic effect (CPE) in both cell lines. The CPE first appeared at 7 days p.i, with detachment of the infected cells from the plastic cell culture plate. At day 9 p.i, we could see a slight change in the morphology of some cells by changing from a flattened to a more rounded up structure. More cells had also detached and the cell monolayer with the infected cells was much less dense than the cell monolayer in the mock-infected wells.

All infection trials were analyzed with two housekeeping genes, 18s and EF1-α, both validated by Jørgensen, S.M, for use as reference genes in real-time PCR reaction studies in Atlantic salmon (Jorgensen, Kleveland et al. 2006). Unfortunately, some of the PCR reactions with 18S showed varying results, with either high C_t-values or poor parallels, and had to be discarded. Relative mRNA transcription levels of the genes were therefore calculated relative to levels in mock-infected cells, and normalized to the expression of EF1-α.

Listed below are the infection trials done on both SHK and ASK. The results from real-time PCR were then exported and analyzed in REST. Graphs were then made from these results by plotting expression levels for every day p.i for each gene in excel.

7.4.1 SHK cells infected with ISAV

SHK cells used in infection trial 1 and 2 had been split between 80 to 90 times (80-90 passages), and the cells used in infection trial 3 and 4 had been split between 50 to 60 times (50-60 passages). After inspection of every PCR-reaction some samples were omitted from the data analysis:

Infection trial 1:

- The component-graphs for the IFN-α reactions showed very low fluorescence compared to background fluorescence, and was therefore discarded.
- The cIAP-1(2) was also discarded for the same reason.

Infection trial 2:

- The component-graphs for the IFN-α reaction showed very low fluorescence compared to background fluorescence, and was therefore discarded.

Infection trial 3:

- One of the parallels for both cIAP-1 and Caspase 3 at day 7 was deleted.

Infection trial 4:

- One of the parallels for both cIAP-1 and bcl2l at day 7 was deleted.

Possible reasons for these failed reactions may be personal errors like, pipetting errors when loading the 96-well plate, contamination in some of the wells before the real-time PCR or errors during mixing of reagents.

The graphs made in excel based on relative expression levels calculated in REST are displayed below:

Infection trial 1

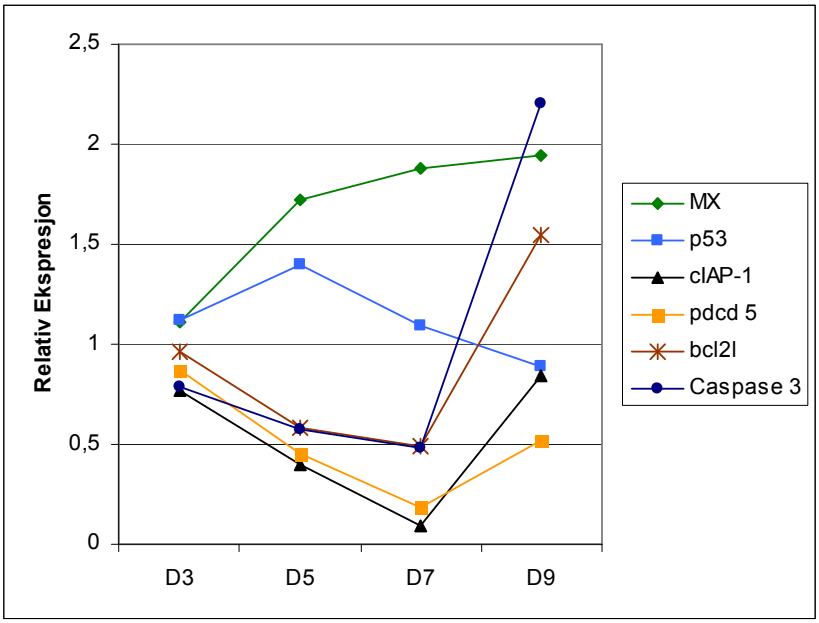

Figure 7.8: Relative expression of MX, p 53, cIAP-1, pdcd 5, Bcl2l and Caspase 3.

Infection trial 2

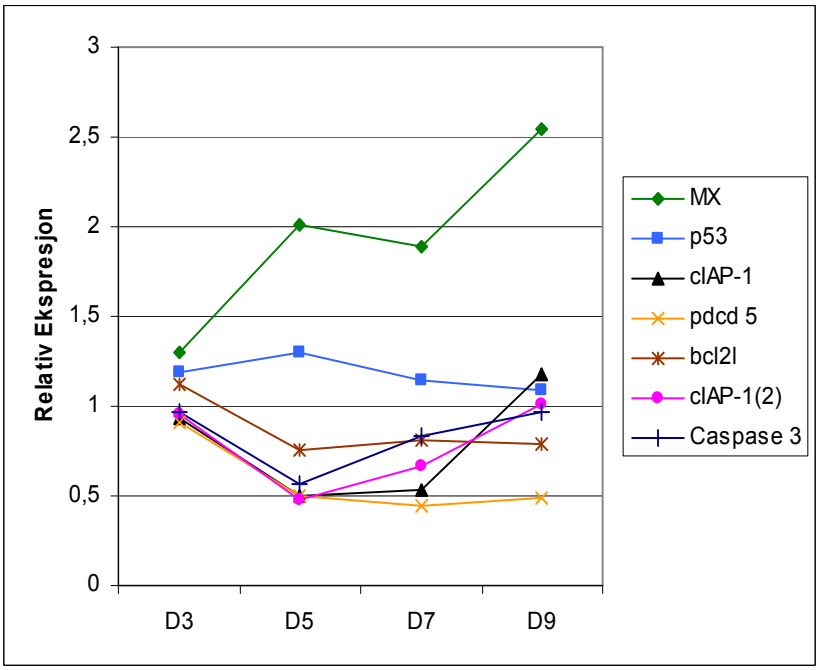

Figure 7.9: Relative expression of MX, p 53, cIAP-1, pdcd 5, Bcl2l , cIAP-1(2) and Caspase 3.

Infection trial 3

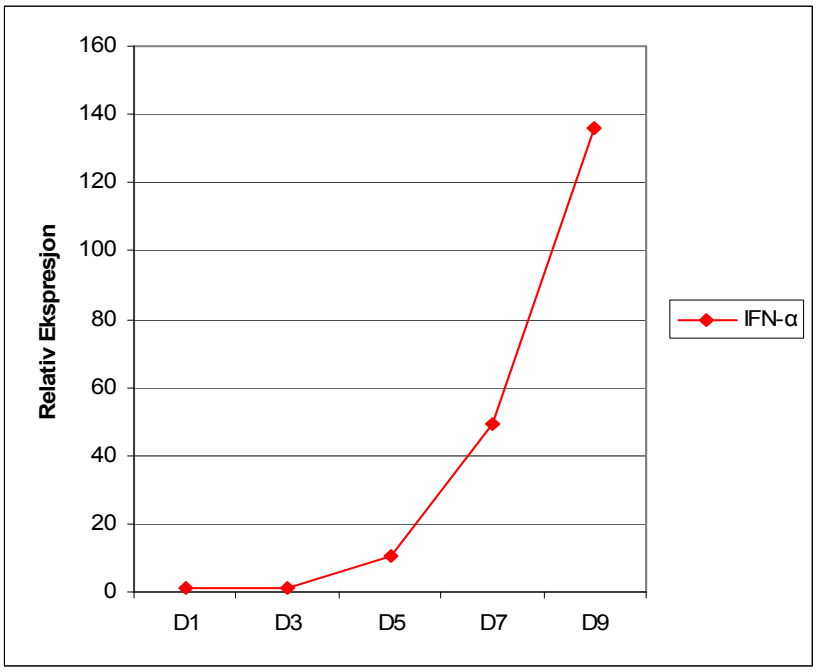

Figure 7.10a: Relative expression of INF α.

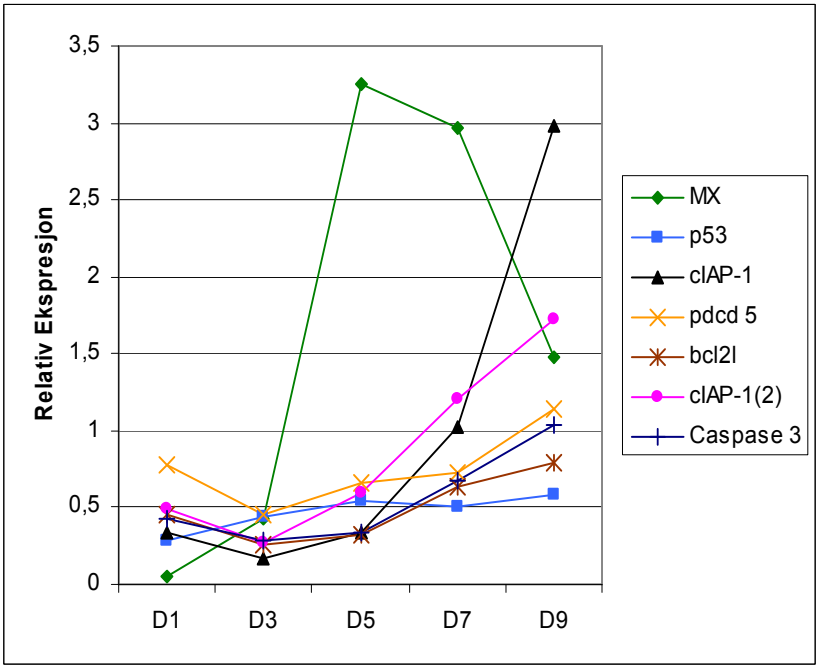

Figure 7.10b: Relative expression of MX, p 53, cIAP-1, pdcd 5, Bcl2l, cIAP-1(2) and Caspase 3.

Infection trial 4

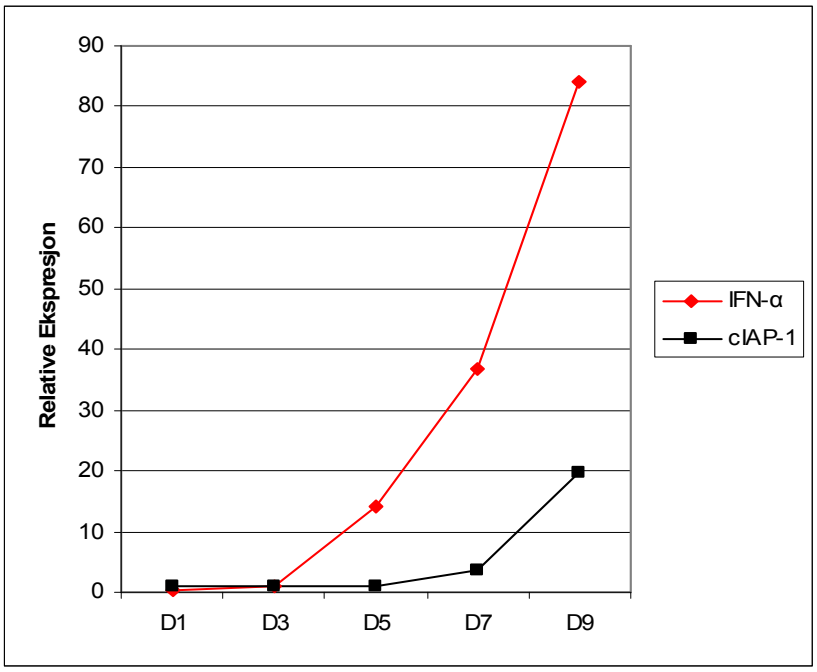

Figure 7.11a: Relative expression of INF α and cIAP-1

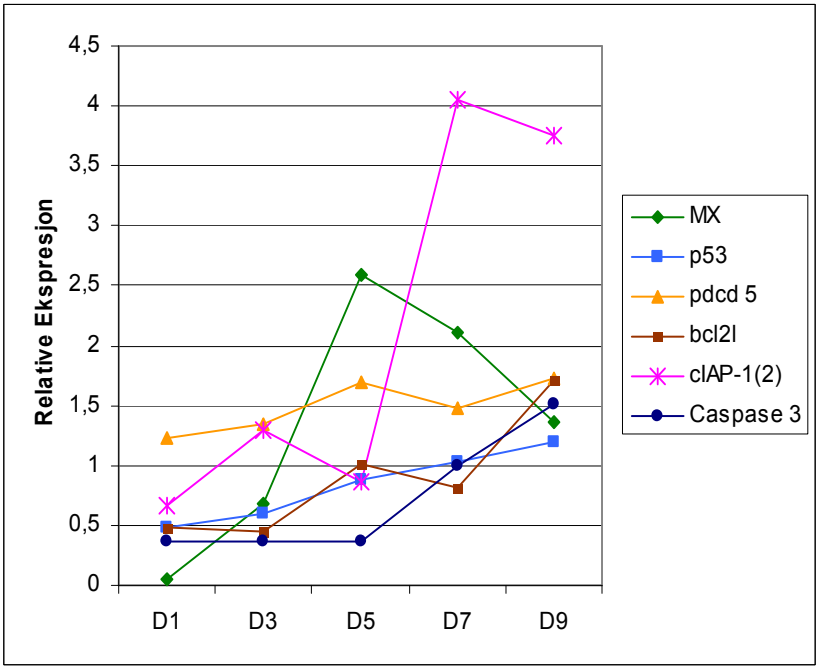

Figure 7.11b: Relative expression of MX, p 53, pdcd5, Bcl2l, cIAP-1(2) and Caspase 3

Summary of results with SHK cells

The relative expression studies (trial 1 and 2) done in cell-lines of high passages (80-90), showed little regulation of the target genes. Previous expression studies done on high passage cell-lines early in this study indicated that cells after a certain amount of passages looses the ability to express and regulate certain genes (data not shown). Rishovd, AL also experienced that the cells used in the early infection trials lost the ability to express some genes (unpublished results). Previous expression studies done in ASK and SHK cell lines have used cells of low passages (40-60) (e.g. (Fast, Ross et al. 2005; Jorgensen, Lyng-Syvertsen et al. 2006)), and thus seems to be of some importance to cell gene expression ability. Compared to the expression results obtained from cells of lower passages, there is a clear loss of expression and regulation in these cells and the results from trial 1 and 2 will therefore not be analyzed any further. Cells with lower passages are also more susceptible to infection.

The relative expression studies done on cells of lower passages (50-60), showed more regulation of the target genes in response to ISAV infection. Figure 7.12 shows the mean relative expression and standard deviations of infection trials 3 and 4, at day 7 post infection.

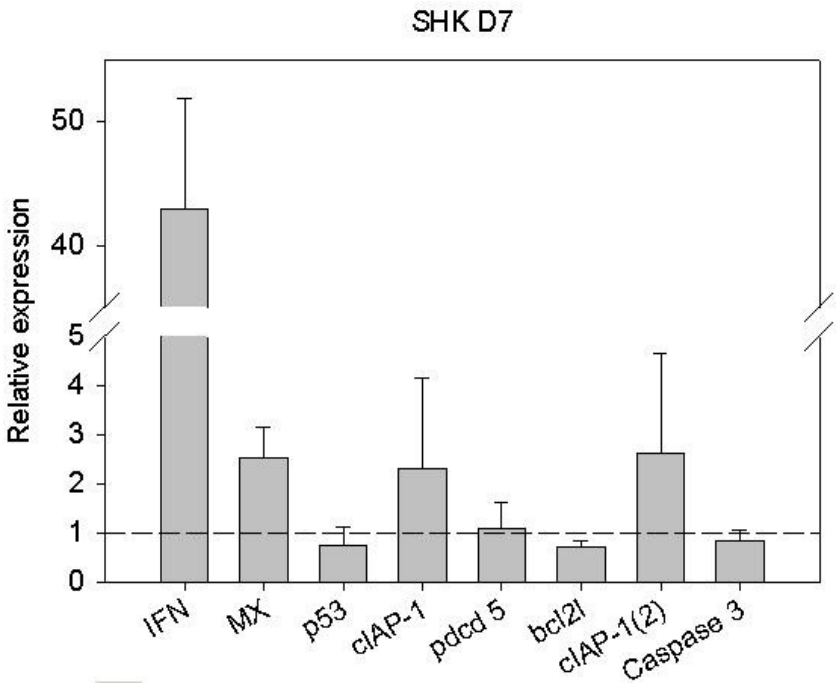

Figure 7.12: Relative expression of target genes in SHK cells at day 7 p.i. Expression is calculated in REST relative to mock-infected cells and normalized to EF1-α.

Day 7 p.i was chosen because of the general mRNA shut-off induced by ISAV under these experimental conditions (Jorgensen, Lyng-Syvertsen et al. 2006). This is a crucial point because real-time PCR data are normalized against housekeeping genes that are influenced by this shut-off and this will likely affect the results of target gene quantification. To ensure that the cell still exhibits a normal gene expression and regulation, and that the mRNA shut-off not had gone too far we focused on the results at day 7 p.i.

All infection trials showed a general down regulation of mRNA levels as the days of infection proceeded. Cycle threshold values (Ct) typically increased 2-4 values from day 1 to day 9 for all the genes (data not shown).

When looking at the net regulation compared to the uninfected samples using EF1-α as a calibrator, IFN-α increased strongly from day one to a 42 fold unregulated level at day 7 post infection.

As a result of this, an induction of the IFN-inducible antiviral Mx gene was also observed at day 7 p.i, to a 2,5 fold level compared to uninfected samples.
Both primer pairs (named cIAP-1 and cIAP-1(2)) for the cIAP-1 gene, resulted in a net up regulation of gene expression to a 2 and 2,2 fold increase in expression respectively. None of the other genes seems to be either up or down regulated to a significant extent.
Although the results above are not statistically significant, due to small sample size, the results strongly indicate an up regulation of IFN, Mx and cIAP-1.

7.4.2 ASK cells infected with ISAV

ASK cells used in infection trial 1 had been split between 110 to 120 times (110-120 passages), and the cells used in infection trial 2 and 3 had been split between 55 to 65 times (55-65 passages). After inspection of every PCR-reaction some samples were omitted from the data analysis:

Infection trial 1:

- The parallels for IFN-α at day 7 were discarded because of poor parallels.

Infection trial 2:

- The component-graphs for the MX reactions in the control showed very low fluorescence compared to background fluorescence. Because relative mRNA transcription levels are calculated relative to levels in the mock-infected cells (control), all MX reactions had to be discarded.

Infection trial 3:

- All reactions showed high fluorescence, good parallels and low Ct-values. None were discarded.

Possible reasons for these failed reactions may be personal errors like, pipetting errors when loading the 96-well plate, contamination in some of the wells before the real-time PCR or errors during mixing of reagents.

The graphs made in excel based on relative expression results calculated in REST are displayed below:

Infection trial 1

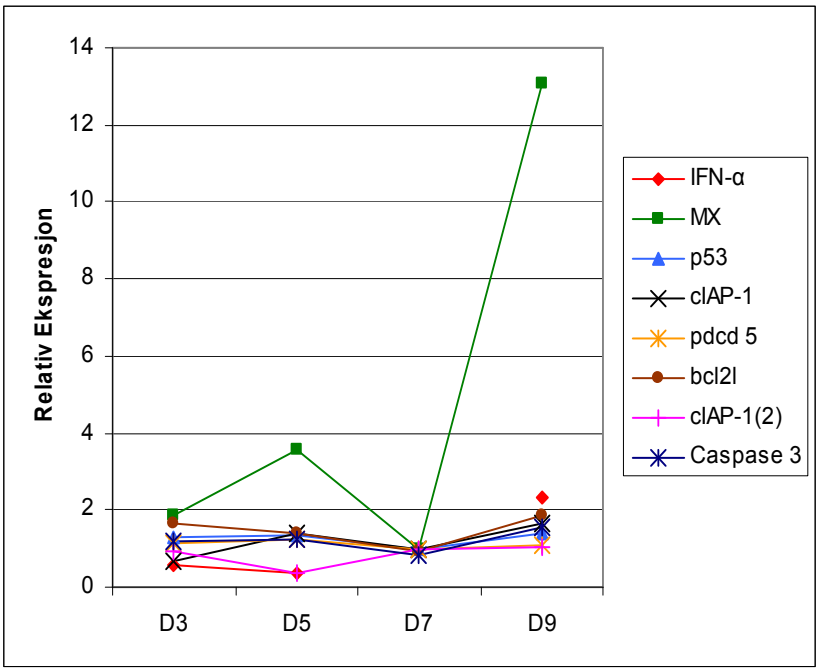

Figure 7.13: Relative expression of IFN α, MX, p 53, cIAP-1, pdcd5, Bcl2l, cIAP-1(2) and Caspase 3

Infection trial 2

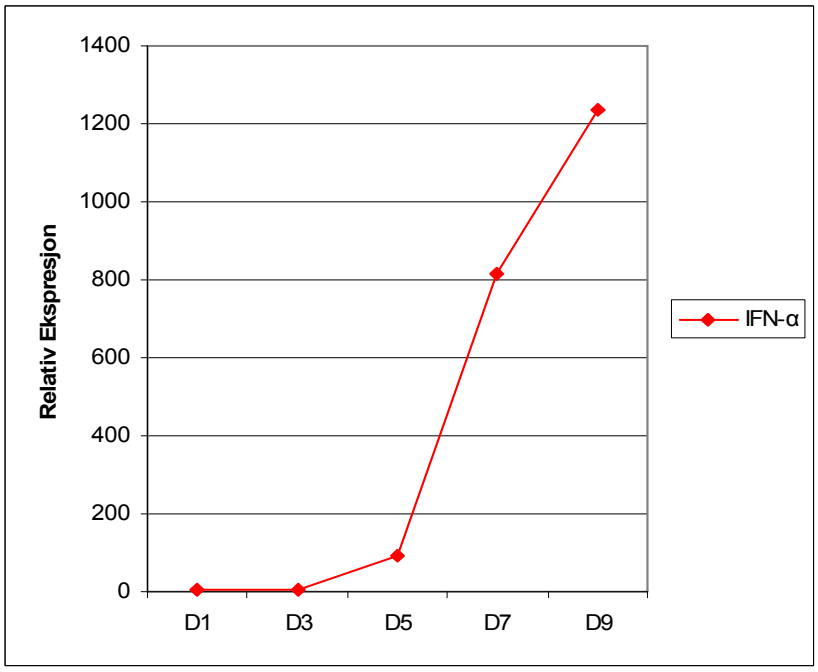

Figure 7.14a: Relative expression of IFN α

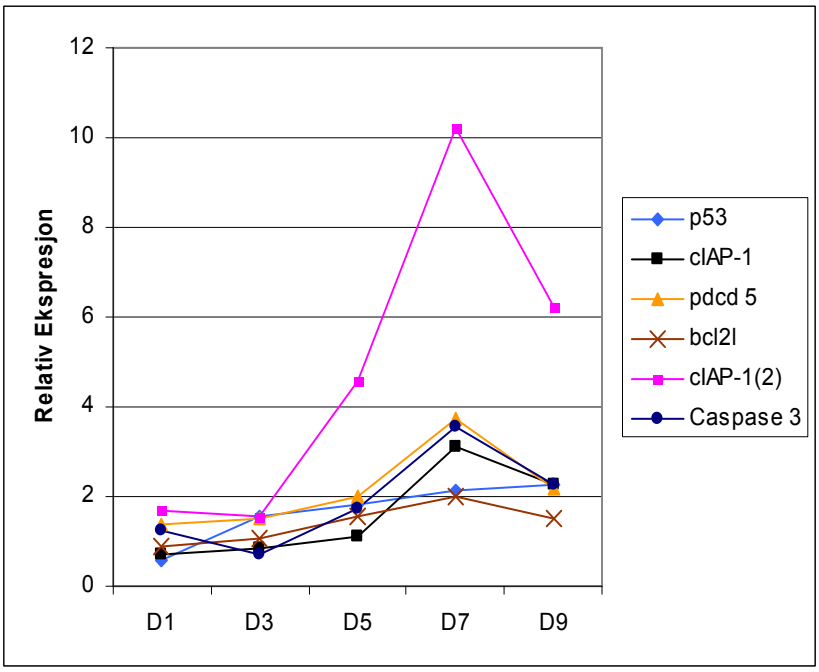

Figure 7.14b: Relative expression of p 53, cIAP-1, pdcd 5, Bcl2l, cIAP-1(2) and Caspase 3.

Infection trial 3

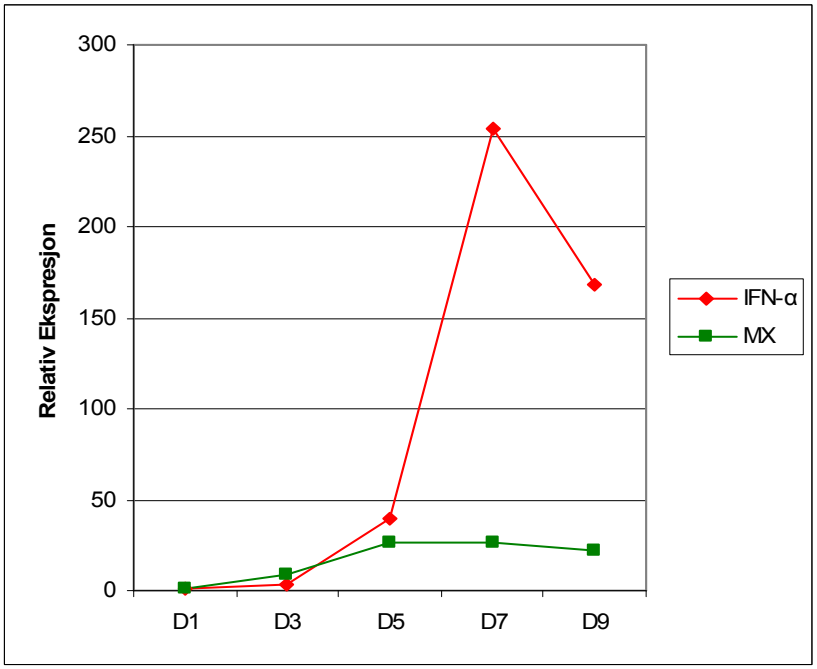

Figure 7.15a: Relative expression of IFN α and MX.

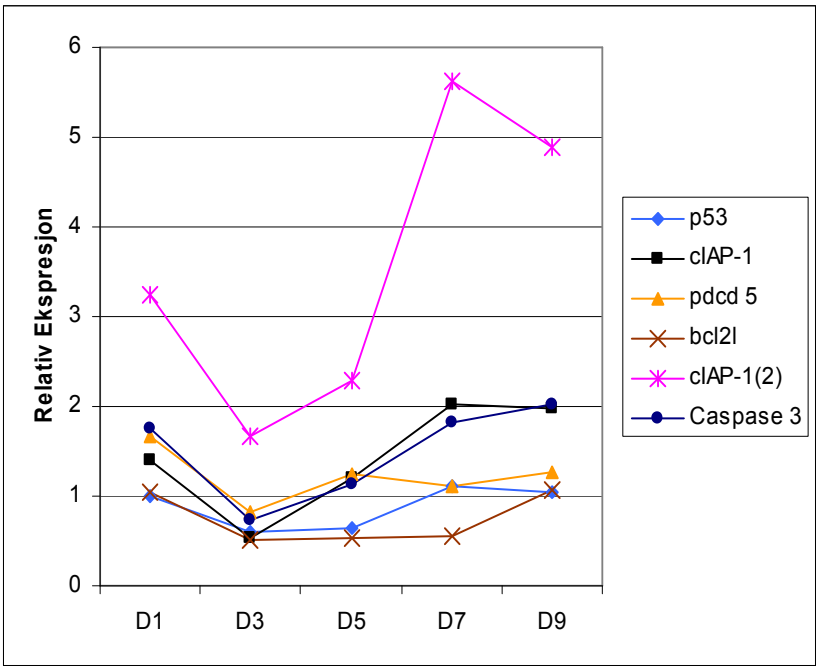

Figure 7.15b: Relative expression of p 53, cIAP-1, pdcd 5, Bcl2l, cIAP-1(2) and Caspase 3.

Summary of results with ASK cells

As with the SHK infection trial, the relative expression studies (trial 1) done in cell-lines of high passages (110-120), showed little regulation of the target genes, and will therefore not be analyzed any further.

The relative expression studies done on cells of lower passages (55-65), showed more regulation of the target genes in response to ISAV infection. Figure 7.16 and 7.17 shows the mean relative expression and standard deviations of infection trials 2 and 3, at day 7 post infection.

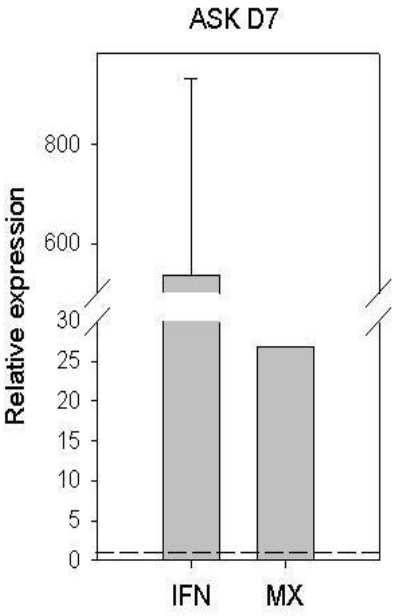

Figure 7.16: Relative expression of IFN-α and Mx in SHK cells at day 7 p.i. Expression is calculated in REST relative to mock-infected cells and normalized to EF1-α.

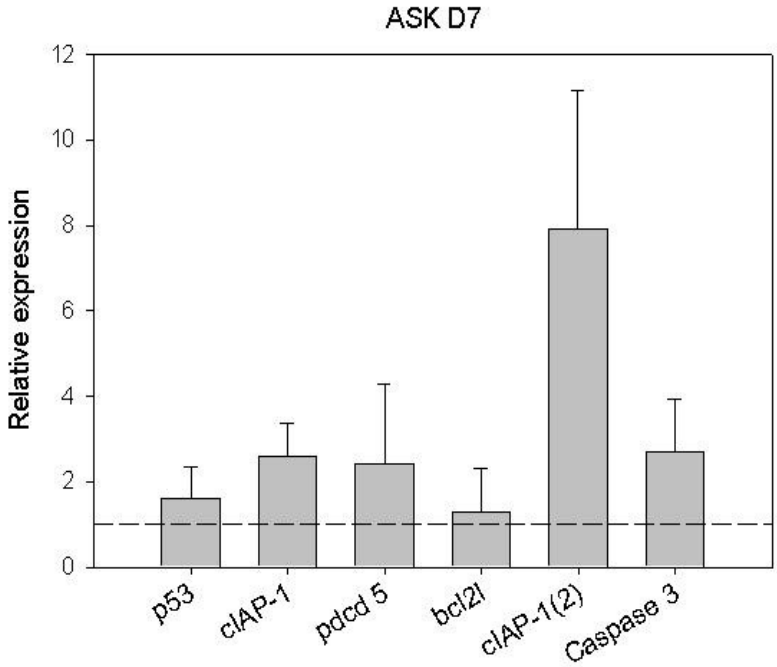

Figure 7.17: Relative expression of target genes in SHK cells at day 7 p.i. Expression is calculated in REST relative to mock-infected cells and normalized to EF1-α.

7 days post infection was chosen for the same reasons discussed in section 7.3.1. These results will also be more comparable to the data obtained in SHK cells when analyzed at the same time post infection.

A general mRNA shut-off was also observed in ASK cells as the infection proceeded. Cycle threshold values (Ct) typically increased 2-4 values from day 1 to day 9 for all the genes, which is normal during infection (data not shown).

When looking the net regulation of gene expression in cells 7 days post infection compared to the uninfected samples and normalized to EF1-α, a strong up regulation of IFN is observed (535 fold up regulation). This high number is due to high differences in relative expression of IFN between the two infection trails. Infection trial 2 has a 817 fold up regulation compared to 253 fold up regulation in trial 3. It's not easy to establish why these high aberrations occur, but personal errors before real-time PCR may be one explanation. In spite of these differences, the data clearly indicates an up regulation of IFN.

As a result of this up regulation Mx also have a 26 fold up regulation compared to mock-infected cells. This number is only taken from one infection trial, because the Mx reactions were discarded from trial 2, and figure 7.16 therefore shows no standard deviation.

Both primer pairs (named cIAP-1 and cIAP-1(2)) for the cIAP-1 gene, resulted in a net up regulation of gene expression to a 2,5 and 8 fold increase in expression respectively. This corresponds well to the up regulation already seen in SHK cells.

In ASK cells both pdcd5 and Caspase 3 also had a slight up regulation of 2,4 and 2,6 respectively. Pdcd5 only show up regulation in infection trial 2, and no up regulation in trial 3, which might indicate the up regulation in trial 2 is due to personal errors. Caspase 3 on the other hand shows a slight up regulation in both infection trials. All though this does not correspond to the results from SHK cells, it might indicate that caspase3 is up regulated in ASK cells.

Although the results above are not statistically significant, due to small sample size, the results strongly indicate an up regulation of IFN, Mx and cIAP-1.

8. DISCUSSION

Apoptosis is a genetically controlled process of cell suicide in response to a variety of stimuli. Apoptosis is considered a part of the innate immune response to virus infection, limiting the time and cellular machinery available for viral replication (Thompson 1995). There are several ways by which viruses might activate the apoptotic pathway. Some viruses do so through direct action of specific viral proteins, such as adenovirus E1A protein (Roulston, Marcellus et al. 1999). Other viruses induce apoptosis indirectly through their effects on cellular functions, for example by shutting down protein synthesis (Hasnain, Begum et al. 2003) or by activating pro-apoptotic proteins, such as upregulation of Fas which can be activated by the dsRNA-activated PKR during influenza virus infection (Balachandran, Roberts et al. 2000).

Previous studies have shown that several RNA viruses induce apoptosis in host-cells. Influenza virus infection induces apoptosis in many cell types, e.g. HeLa and Madin-Darby canine kidney (MDCK) cells, lymphocytes, neutrophils and bronchiolar epithelial cells (Brydon, Smith et al. 2003). Infectious pancreatic necrosis virus induces apoptosis in cultured fish cells (Santi, Sandtro et al. 2005). A recent study also suggests that the CPE observed in ISAV-infected SHK-1 and CHSE-214 cells is associated with apoptosis (Joseph, Cepica et al. 2004).

Studies of ISAV-induced apoptosis may provide a clearer picture of the cellular mechanisms of viral persistence and pathogenesis in ISAV infection.
In the present study we wanted to investigate the effect of ISAV infection on the expression of apoptosis related genes in Atlantic salmon (*Salmo Salar L.*) cells. By using a quantitative real-time PCR approach we analyzed the regulation of key apoptosis related genes during ISAV infection *in vitro.* Two different permissive fish cell lines for ISAV were used in this study, Atlantic salmon head kidney (ASK) cells (Rolland, Bouchard et al. 2005) and salmon head kidney (SHK-1) cells (Dannevig, Falk et al. 1995), which are macrophage-like cell lines in which virus replicates with production of cytopathic effect (CPE).

Both ASK and SHK cells were infected with a low MOI (0,025) of ISAV and may have caused infection in relatively few cells initially. This implied that the increase in viral

mRNA results from increased transcription in these few cells. Because of this some of the initial changes in transcriptional activity in the cells analyzed might reflect cell responses to interferon signalling and not virus effects. However, in the late phase of the infection we could see an increased viral transcription (200-fold at day 7 p.i) and there was a clear shut-off of cellular RNA synthesis induced by ISAV. Based on this, and to make sure the RNA shut-off not had gone too far, we decided to analyze our data from the viral infections at day 7 p.i.

The ideal reference gene should be expressed in an unchanging fashion regardless off experimental conditions, including different tissues or cell types, developmental stage, or sample treatment. Because there is no one gene that meets this criterion for every experimental condition, it is necessary to validate the expression stability of a control gene for the specific requirements of an experiment prior to its use for normalization (Wong and Medrano 2005). The reference gene used in this study, EF1-α, has already been validated for real-time PCR reaction studies in Atlantic salmon (Jorgensen, Kleveland et al. 2006). A previous study (Jorgensen, Lyng-Syvertsen et al. 2006) has shown that the relative expression levels of EF1-α during infection were 2,5-5,5 fold down regulated, at day 7 p.i, due to the mRNA shut-off by ISAV. This means that by normalizing data using EF1-α as a reference gene we can estimate the virus-induced effect on target genes relative to the housekeeping transcriptome. In other words, a target gene that is less down regulated than the reference gene, when normalized against the reference gene, can be considered up regulated.

As expected, a strong IFN-α response was observed in both ASK and SHK cells in response to the ISAV infection, in line with observations from other salmon cell lines (Jensen, Albuquerque et al. 2002). In light of the low MOI used, this rapid and strong induction of IFN and the resulting induction of Mx demonstrated high sensitivity for low doses of viral RNA.

Previous infection studies with influenza A virus, have also demonstrated an early up regulation of IFN- inducible genes even at a MOI of 0,1, suggesting that the expression of these genes may be important in initiating the cascade of an antiviral response (Tong, Long et al. 2004).

No antiviral effect of Mx was evident in either ASK or SHK cells and the transcription of ISAV mRNA (segment 5) increased steadily (figure 7.5) throughout the infection despite of elevated Mx mRNA levels (figure 7.10 and 7.14). In addition, mRNA shut-off was increasing, indicating that IFN and Mx were unable to block viral replication and recover host cell RNA synthesis. This supports previous reports and no antiviral effect of Mx has so far

been demonstrated against ISAV in Atlantic salmon cells (Jensen and Robertsen 2002), in contrast to what has been observed in Chinook salmon CHSE cells (Kibenge, Munir et al. 2005).

The IAP-family and their ability to inhibit apoptosis has been reviewed in (Deveraux and Reed 1999). First discovered in bacloviruses, IAPs were shown to be involved in the suppression of the host cell death response to viral infection (Crook, Clem et al. 1993). cIAP, which is a gene encoding the inhibitor of apoptosis protein, was also up regulated in both cell lines in response to ISAV infection. A slight up regulation of some genes in the IAP-family have also been demonstrated during influenza A infection, but then at a MOI of 1,0 (Tong, Long et al. 2004).

Apoptosis is mainly thought to be a process initiated by the host cell to limit the time and cellular machinery available for viral replication (Thompson 1995). Many RNA viruses, including ISAV (Joseph, Cepica et al. 2004), are known to induce apoptosis under conditions which allow efficient virus multiplication (i.e, a permissive infection). A study (Koyama, Fukumori et al. 2000) demonstrated that, by rapid multiplication, influenza viruses and probably many other RNA viruses are able to complete viral replication long before the onset of virus induced apoptosis, and thereby cause a permissive infection.

The up regulation of cIAP, as a result of the ISAV infection, might therefore be a mechanism by which the virus post-pone the apoptotic process in the host cell, to ensure more time for viral replication.

Adenoviruses have previously been shown to delay apoptosis in cerebellar granule neurons, through actions involving IAPs (Simons, Beinroth et al. 1999).

The ASK cells also showed a tendency to up regulate the expression of caspase 3. This was not observed in the SHK-1 cell line.

Caspase is a central player in apoptosis regulation and its activity is often measured to determine the impact of a given apoptotic stimulus (Watanabe, Hitomi et al. 2002). A recent study demonstrated that caspase-3 activation is essential for influenza A virus propagation in cell cultures (Wurzer, Planz et al. 2003). On the other hand, Joseph *et al.* (2004) has studied ISAV-induced apoptosis and suggested that ISAV-induced apoptosis in SHK-1 cells occurs via the caspase-activation pathway, but may not involve activation of caspase-3. If our results show an up regulation of caspase-3 in ASK cells or if the up regulation is due to personal errors, is hard to say.

Even though one genes expression is up regulated, it might not have a biological effect on the cell, as it is the proteins that exert the effects in a cell. Caspases and p53 are for example thought to have a constant expression in the cell, and is mainly regulated at the protein level through switching form an inactivated to an activated state (Alberts, Johnson et al. 2002). All these results therefore, only give indications of what the cell responses are to the viral infection.

9. CONCLUSION

In this study, were we investigated the gene expression of several apoptosis related genes in response to ISAV infection, our results strongly indicate an up regulation of IFN-α, Mx and cIAP-1, in both ASK and SHK-1 cell lines.

In light of the low MOI used in this study, the rapid and strong induction of IFN-α demonstrates that the cells are highly sensitive to low doses of viral RNA.

Our results also show that the strong induction of IFN-α and Mx does not affect the transcription of viral mRNA, as it increased steadily throughout the infection. This indicates that these genes have little or no antiviral effect against ISAV in Atlantic salmon cells.

10. REFERECES

Alberts, B., A. Johnson, et al. (2002). Programmed cell death (Apoptosis). Molecular Biology of The Cell. Garland Science, Taylor & Francis Group, New York**:** 1010-1026.

Aspehaug, V., A. B. Mikalsen, et al. (2005). "Characterization of the infectious salmon anemia virus fusion protein." J Virol **79**(19): 12544-53.

Balachandran, S., P. C. Roberts, et al. (2000). "Alpha/beta interferons potentiate virus-induced apoptosis through activation of the FADD/Caspase-8 death signaling pathway." J Virol **74**(3): 1513-23.

Battaglia, M., P. Pedrazzoli, et al. (1998). "Epithelial tumour cell detection and the unsolved problems of nested RT-PCR: a new sensitive one step method without false positive results." Bone Marrow Transplant **22**(7): 693-8.

Bonjardim, C. A. (2005). "Interferons (IFNs) are key cytokines in both innate and adaptive antiviral immune responses--and viruses counteract IFN action." Microbes Infect **7**(3): 569-78.

Bouchard, D., W. Keleher, et al. (1999). "Isolation of infectious salmon anemia virus (ISAV) from Atlantic salmon in New Brunswick, Canada." Dis Aquat Organ **35**(2): 131-7.

Brydon, E. W., H. Smith, et al. (2003). "Influenza A virus-induced apoptosis in bronchiolar epithelial (NCI-H292) cells limits pro-inflammatory cytokine release." J Gen Virol **84**(Pt 9): 2389-400.

Bustin, S. A. (2000). "Absolute quantification of mRNA using real-time reverse transcription polymerase chain reaction assays." J Mol Endocrinol **25**(2): 169-93.

Chang, Y. F., C. M. Cheng, et al. (2006). "The F-box protein Fbxo7 interacts with human inhibitor of apoptosis protein cIAP1 and promotes cIAP1 ubiquitination." Biochem Biophys Res Commun **342**(4): 1022-6.

Chen, M. C., H. Y. Gong, et al. (2001). "Cloning and characterization of zfBLP1, a Bcl-XL homologue from the zebrafish, Danio rerio." Biochim Biophys Acta **1519**(1-2): 127-33.

Chen, W., P. A. Calvo, et al. (2001). "A novel influenza A virus mitochondrial protein that induces cell death." Nat Med **7**(12): 1306-12.

Chen, Y., R. Sun, et al. (2001). "Nuclear translocation of PDCD5 (TFAR19): an early signal for apoptosis?" FEBS Lett **509**(2): 191-6.

Clouthier, S. C., T. Rector, et al. (2002). "Genomic organization of infectious salmon anaemia virus." J Gen Virol **83**(Pt 2): 421-428.

Cox, R. J., K. A. Brokstad, et al. (2004). "Influenza virus: immunity and vaccination strategies. Comparison of the immune response to inactivated and live, attenuated influenza vaccines." Scand J Immunol **59**(1): 1-15.

Crook, N. E., R. J. Clem, et al. (1993). "An apoptosis-inhibiting baculovirus gene with a zinc finger-like motif." J Virol **67**(4): 2168-74.

Dannevig, B. H., K. Falk, et al. (1995). "Isolation of the causal virus of infectious salmon anaemia (ISA) in a long-term cell line from Atlantic salmon head kidney." J Gen Virol **76 (Pt 6)**: 1353-9.

Dannevig, B. H., K. Falk, et al. (1995). "Propagation of infectious salmon anaemia (ISA) virus in cell culture." Vet Res **26**(5-6): 438-42.

Degterev, A., M. Boyce, et al. (2003). "A decade of caspases." Oncogene **22**(53): 8543-67.

Deveraux, Q. L. and J. C. Reed (1999). "IAP family proteins--suppressors of apoptosis." Genes Dev **13**(3): 239-52.

Devold, M., B. Krossoy, et al. (2000). "Use of RT-PCR for diagnosis of infectious salmon anaemia virus (ISAV) in carrier sea trout Salmo trutta after experimental infection." Dis Aquat Organ **40**(1): 9-18.

Falk, K., V. Aspehaug, et al. (2004). "Identification and characterization of viral structural proteins of infectious salmon anemia virus." J Virol **78**(6): 3063-71.

Falk, K., E. Namork, et al. (1998). "Characterization and applications of a monoclonal antibody against infectious salmon anaemia virus." Dis Aquat Organ **34**(2): 77-85.

Fast, M. D., N. W. Ross, et al. (2005). "Prostaglandin E(2) modulation of gene expression in an Atlantic salmon (Salmo salar) macrophage-like cell line (SHK-1)." Dev Comp Immunol **29**(11): 951-63.

Gibson, U. E., C. A. Heid, et al. (1996). "A novel method for real time quantitative RT-PCR." Genome Res **6**(10): 995-1001.

Gil, J. and M. Esteban (2000). "Induction of apoptosis by the dsRNA-dependent protein kinase (PKR): mechanism of action." Apoptosis **5**(2): 107-14.

Ginzinger, D. G. (2002). "Gene quantification using real-time quantitative PCR: an emerging technology hits the mainstream." Exp Hematol **30**(6): 503-12.

Gross, A., J. M. McDonnell, et al. (1999). "BCL-2 family members and the mitochondria in apoptosis." Genes Dev **13**(15): 1899-911.

Haller, O. and G. Kochs (2002). "Interferon-induced mx proteins: dynamin-like GTPases with antiviral activity." Traffic **3**(10): 710-7.

Hasnain, S. E., R. Begum, et al. (2003). "Host-pathogen interactions during apoptosis." J Biosci **28**(3): 349-58.

Heid, C. A., J. Stevens, et al. (1996). "Real time quantitative PCR." Genome Res **6**(10): 986-94.

Jensen, I., A. Albuquerque, et al. (2002). "Effect of poly I:C on the expression of Mx proteins and resistance against infection by infectious salmon anaemia virus in Atlantic salmon." Fish Shellfish Immunol **13**(4): 311-26.

Jensen, I. and B. Robertsen (2002). "Effect of double-stranded RNA and interferon on the antiviral activity of Atlantic salmon cells against infectious salmon anemia virus and infectious pancreatic necrosis virus." Fish Shellfish Immunol **13**(3): 221-41.

Johnstone, R. W., A. A. Ruefli, et al. (2002). "Apoptosis: a link between cancer genetics and chemotherapy." Cell **108**(2): 153-64.

Jorgensen, S. M., E. J. Kleveland, et al. (2006). "Validation of reference genes for real-time polymerase chain reaction studies in atlantic salmon." Mar Biotechnol (NY) **8**(4): 398-408.

Jorgensen, S. M., B. Lyng-Syvertsen, et al. (2006). "Expression of MHC class I pathway genes in response to infectious salmon anaemia virus in Atlantic salmon (Salmo salar L.) cells." Fish Shellfish Immunol **21**(5): 548-60.

Joseph, T., A. Cepica, et al. (2004). "Mechanism of cell death during infectious salmon anemia virus infection is cell type-specific." J Gen Virol **85**(Pt 10): 3027-36.

Karge, W. H., 3rd, E. J. Schaefer, et al. (1998). "Quantification of mRNA by polymerase chain reaction (PCR) using an internal standard and a nonradioactive detection method." Methods Mol Biol **110**: 43-61.

Kawaoka, Y. (2001). "Influenza Viruses." ENCYCLOPEDIA OF LIFE SCIENCES(John Wiley & Sons, Ltd: Chichester): http://www.els.net/ [DOI: 10.1038/npg.els.0001031].

Kerr, J. F., A. H. Wyllie, et al. (1972). "Apoptosis: a basic biological phenomenon with wide-ranging implications in tissue kinetics." Br J Cancer **26**(4): 239-57.

Kibenge, F. S., O. N. Garate, et al. (2001). "Isolation and identification of infectious salmon anaemia virus (ISAV) from Coho salmon in Chile." Dis Aquat Organ **45**(1): 9-18.

Kibenge, F. S., K. Munir, et al. (2004). "Infectious salmon anemia virus: causative agent, pathogenesis and immunity." Anim Health Res Rev **5**(1): 65-78.

Kibenge, M. J., K. Munir, et al. (2005). "Constitutive expression of Atlantic salmon Mx1 protein in CHSE-214 cells confers resistance to infectious salmon anaemia virus." Virol J **2**: 75.

Koyama, A. H., T. Fukumori, et al. (2000). "Physiological significance of apoptosis in animal virus infection." Microbes Infect **2**(9): 1111-7.

Krammer, P. H. (2000). "CD95's deadly mission in the immune system." Nature **407**(6805): 789-95.

Kroemer, G. and J. C. Reed (2000). "Mitochondrial control of cell death." Nat Med **6**(5): 513-9.

Krossoy, B., I. Hordvik, et al. (1999). "The putative polymerase sequence of infectious salmon anemia virus suggests a new genus within the Orthomyxoviridae." J Virol **73**(3): 2136-42.

Lamb, R. A., and Krug, R.M (2001). Orthomyxoviridae: The virus and their replication. Philadelphia, Lippincott William & Wilkins.

Leahy, M. B., J. T. Dessens, et al. (1997). "The fourth genus in the Orthomyxoviridae: sequence analyses of two Thogoto virus polymerase proteins and comparison with influenza viruses." Virus Res **50**(2): 215-24.

Lekanne Deprez, R. H., A. C. Fijnvandraat, et al. (2002). "Sensitivity and accuracy of quantitative real-time polymerase chain reaction using SYBR green I depends on cDNA synthesis conditions." Anal Biochem **307**(1): 63-9.

Lin, D. A., S. Roychoudhury, et al. (1991). "Evolutionary relatedness of the predicted gene product of RNA segment 2 of the tick-borne Dhori virus and the PB1 polymerase gene of influenza viruses." Virology **182**(1): 1-7.

Liu, W. and D. A. Saint (2002). "A new quantitative method of real time reverse transcription polymerase chain reaction assay based on simulation of polymerase chain reaction kinetics." Anal Biochem **302**(1): 52-9.

Livak, K. J. and T. D. Schmittgen (2001). "Analysis of relative gene expression data using real-time quantitative PCR and the 2(-Delta Delta C(T)) Method." Methods **25**(4): 402-8.

Lovely, J. E., B. H. Dannevig, et al. (1999). "First identification of infectious salmon anaemia virus in North America with haemorrhagic kidney syndrome." Dis Aquat Organ **35**(2): 145-8.

Mannherz, H. G., S. M. Gonsior, et al. (2006). "Dual effects of staurosporine on A431 and NRK cells: microfilament disassembly and uncoordinated lamellipodial activity followed by cell death." Eur J Cell Biol **85**(8): 785-802.

Martin, S. J., C. P. Reutelingsperger, et al. (1995). "Early redistribution of plasma membrane phosphatidylserine is a general feature of apoptosis regardless of the initiating stimulus: inhibition by overexpression of Bcl-2 and Abl." J Exp Med **182**(5): 1545-56.

Meier, P., A. Finch, et al. (2000). "Apoptosis in development." Nature **407**(6805): 796-801.

Mjaaland, S., E. Rimstad, et al. (1997). "Genomic characterization of the virus causing infectious salmon anemia in Atlantic salmon (Salmo salar L.): an orthomyxo-like virus in a teleost." J Virol **71**(10): 7681-6.

Morris, S. J., G. E. Price, et al. (1999). "Role of neuraminidase in influenza virus-induced apoptosis." J Gen Virol **80 (Pt 1)**: 137-46.

Munir, K. and F. S. Kibenge (2004). "Detection of infectious salmon anaemia virus by real-time RT-PCR." J Virol Methods **117**(1): 37-47.

Müllauer, L. (2006). "Apoptosis: Regulatory Genes and Disease " ENCYCLOPEDIA OF LIFE SCIENCES(John Wiley & Sons, Ltd: Chichester): http://www.els.net/ [DOI: 10.1002/9780470015902.a0006044].

Penny, R. and R. Stuart-Harris (2001). "Interferons: Therapeutic Uses." ENCYCLOPEDIA OF LIFE SCIENCES(John Wiley & Sons, Ltd: Chichester): http://www.els.net/ [DOI: 10.1038/npg.els.0002168].

Pfaffl, M. W., G. W. Horgan, et al. (2002). "Relative expression software tool (REST) for group-wise comparison and statistical analysis of relative expression results in real-time PCR." Nucleic Acids Res **30**(9): e36.

Pringle, C. R. (1996). "Virus taxonomy 1996 - a bulletin from the Xth International Congress of Virology in Jerusalem." Arch Virol **141**(11): 2251-6.

Rasmussen, R. (2001). Quantification on the LightCycler. C. T. W. *In* S. Meuer, and K. Nakagawara (Eds.), Rapid Cycle Real-time PCR, Methodes and Applications. Springer Press, Heidelberg.**:** 21-34.

Reed, J. C. (2000). "Mechanisms of apoptosis." Am J Pathol **157**(5): 1415-30.

Reinhold, U., C. Berkin, et al. (2001). "Interlaboratory evaluation of a new reverse transcriptase polymerase chain reaction-based enzyme-linked immunosorbent assay for the detection of circulating melanoma cells: a multicenter study of the Dermatologic Cooperative Oncology Group." J Clin Oncol **19**(6): 1723-7.

Rimstad, E. and S. Mjaaland (2002). "Infectious salmon anaemia virus." Apmis **110**(4): 273-82.

Rimstad, E., S. Mjaaland, et al. (2001). "Characterization of the infectious salmon anemia virus genomic segment that encodes the putative hemagglutinin." J Virol **75**(11): 5352-6.

Ririe, K. M., R. P. Rasmussen, et al. (1997). "Product differentiation by analysis of DNA melting curves during the polymerase chain reaction." Anal Biochem **245**(2): 154-60.

Ritchie, R. J., A. Bardiot, et al. (2002). "Identification and characterisation of the genomic segment 7 of the infectious salmon anaemia virus genome." Virus Res **84**(1-2): 161-70.

Ritchie, R. J., J. Heppell, et al. (2001). "Identification and characterization of segments 3 and 4 of the ISAV genome." Virus Genes **22**(3): 289-97.

Rolland, J. B., D. Bouchard, et al. (2005). "Combined use of the ASK and SHK-1 cell lines to enhance the detection of infectious salmon anemia virus." J Vet Diagn Invest **17**(2): 151-7.

Roulston, A., R. C. Marcellus, et al. (1999). "Viruses and apoptosis." Annu Rev Microbiol **53**: 577-628.

Samuel, C. E. (2001). "Antiviral actions of interferons." Clin Microbiol Rev **14**(4): 778-809, table of contents.

Santi, N., A. Sandtro, et al. (2005). "Infectious pancreatic necrosis virus induces apoptosis in vitro and in vivo independent of VP5 expression." Virology **342**(1): 13-25.

Schultz-Cherry, S., N. Dybdahl-Sissoko, et al. (2001). "Influenza virus ns1 protein induces apoptosis in cultured cells." J Virol **75**(17): 7875-81.

Simons, M., S. Beinroth, et al. (1999). "Adenovirus-mediated gene transfer of inhibitors of apoptosis protein delays apoptosis in cerebellar granule neurons." J Neurochem **72**(1): 292-301.

Snow, M., P. McKay, et al. (2006). "Development, application and validation of a Taqman real-time RT-PCR assay for the detection of infectious salmon anaemia virus (ISAV) in Atlantic salmon (Salmo salar)." Dev Biol (Basel) **126**: 133-45; discussion 325-6.

Snow, M., R. S. Raynard, et al. (2003). "An evaluation of current diagnostic tests for the detection of infectious salmon anaemia virus (ISAV) following experimental water-borne infection of Atlantic salmon, Salmo salar L." J Fish Dis **26**(3): 135-45.

Thompson, C. B. (1995). "Apoptosis in the pathogenesis and treatment of disease." Science **267**(5203): 1456-62.

Thorud, K. E. and H. O. Djupvik (1988). "Infectious anemia in Atlantic salmon (*Salmo salar L.*)." Bull. Eur. Assoc. Fish Pathol.(8): 109-111.

Tichopad, A., M. Dilger, et al. (2003). "Standardized determination of real-time PCR efficiency from a single reaction set-up." Nucleic Acids Res **31**(20): e122.

Tong, H. H., J. P. Long, et al. (2004). "Alteration of gene expression in human middle ear epithelial cells induced by influenza A virus and its implication for the pathogenesis of otitis media." Microb Pathog **37**(4): 193-204.

Vandesompele, J., A. De Paepe, et al. (2002). "Elimination of primer-dimer artifacts and genomic coamplification using a two-step SYBR green I real-time RT-PCR." Anal Biochem **303**(1): 95-8.

Vogelstein, B., D. Lane, et al. (2000). "Surfing the p53 network." Nature **408**(6810): 307-10.

Watanabe, M., M. Hitomi, et al. (2002). "The pros and cons of apoptosis assays for use in the study of cells, tissues, and organs." Microsc Microanal **8**(5): 375-91.

Wittwer, C. T., M. G. Herrmann, et al. (1997). "Continuous fluorescence monitoring of rapid cycle DNA amplification." Biotechniques **22**(1): 130-1, 134-8.

Wong, M. L. and J. F. Medrano (2005). "Real-time PCR for mRNA quantitation." Biotechniques **39**(1): 75-85.

Wu, M. (2001). "Apoptosis: Molecular Mechanisms " ENCYCLOPEDIA OF LIFE SCIENCES(John Wiley & Sons, Ltd: Chichester): http://www.els.net/ [DOI: 10.1038/npg.els.0001150].

Wurzer, W. J., O. Planz, et al. (2003). "Caspase 3 activation is essential for efficient influenza virus propagation." Embo J **22**(11): 2717-28.

Wyllie, A. H. (1980). "Glucocorticoid-induced thymocyte apoptosis is associated with endogenous endonuclease activation." Nature **284**(5756): 555-6.

Zhirnov, O. P., T. E. Konakova, et al. (1999). "Caspase-dependent N-terminal cleavage of influenza virus nucleocapsid protein in infected cells." J Virol **73**(12): 10158-63.

Zhirnov, O. P., A. L. Ksenofontov, et al. (2002). "Interaction of influenza A virus M1 matrix protein with caspases." Biochemistry (Mosc) **67**(5): 534-9.